Applications of Surface Acoustic and Shallow Bulk Acoustic Wave Devices

COLIN K. CAMPBELL, FELLOW, IEEE

Invited Paper

Applications of surface acoustic wave (SAW) and shallow bulk acoustic wave (SBAW) devices are reviewed. SAW-device coverage includes delay lines and filters operating at selected frequencies in the range from about 10 MHz to 11 GHz, modeling with single-crystal piezoelectrics and layered structures, resonators and low-loss filters, comb filters and multiplexers, antenna duplexers, harmonic devices, chirp filters for pulse compression, coding with fixed and programmable transversal filters, Barker and quadraphase coding, adaptive filters, acoustic and acoustoelectric convolvers and correlators for radar, spread spectrum, and packet radio, acoustooptic processors for Bragg modulation and spectrum analysis, real-time Fourier-transform, and cepstrum processors for radar and sonar, compressive receivers, Nyquist filters for microwave digital radio, clock-recovery filters for optical fiber communications, fixed-, tunable-, and multimode-oscillators, and frequency synthesizers, acoustic charge transport (ACT), and other SAW devices for signal processing on gallium arsenide, SAW sensors, and scanning acoustic microscopy.

SBAW-devices applications include gigahertz delay lines, surface transverse wave resonators employing energy-trapping gratings, as well as oscillators with enhanced performance and capability.

I. INTRODUCTION

A. SAW-Device Development

The phenomenon of surface acoustic wave (SAW) propagation was first reported on by Lord Rayleigh in 1885 [1]. It was not until 1965, however, that such wave motion (also known as Rayleigh waves) was efficiently utilized for electronic filter and analog signal-processing applications, by the use of voltage-excited metal-film interdigital transducers (IDTs) on the surface of a piezoelectric substrate [2].

Following this development, consumer electronic interests in SAW devices initially focused on the large-volume, low-cost market for intermediate frequency (IF) filters for domestic TV receivers. Military and commercial developments related to low-volume, high-cost, SAW chirp filters for radar signal processing. This rapidly expanded into a multitude of products and applications, however, in exploiting the capabilities of SAW devices. Mechanical attributes contributing to this expansion are ruggedness, light weight, and small size. Electrical merits feature the ability for signal processing at selected frequencies in the range from about 10 MHz up to a current reported value of 11 GHz [3].

While their circuit use was initially limited to implementation in intermediate frequency (IF) stages with large signal-voltage levels, as dictated by the high values of insertion loss ($\simeq$15–40 dB) inherent in "first generation" SAW devices, much research has been subsequently applied to SAW filters with insertion loss less than $\simeq$3 dB, for low signal-level or receiver front-end filtering. For example, SAW filters with 3–5-W power-handling capabilities are employed in antenna duplexers for mobile telephone transceivers operating at 835 MHz [4]. Also, increasing thrust has been applied to SAW-based signal processing and integrated-circuit compatibility on gallium arsenide (GaAs), which is a piezoelectric as well as a semiconductor.

Overall, the demand for SAW devices has led to a commercial market currently running at a multi-million level in both annual dollar sales and device quantity. Toshiba in Japan now produces about 5 million SAW devices per month, mainly for IF filters and resonators for TV and VCR circuits [5]. To illustrate this rapid growth, Williamson [6], in 1977, reported 45 different types of SAW devices under development, including 10 major devices with widespread application. In 1985, Hartmann [7] subsequently listed nine major commercial applications, nine major consumer applications, and 18 major military applications of SAW technology. Highlights of SAW-based device applications are given in Table 1.

Extensive development of shallow bulk acoustic wave (SBAW) devices has also been under way since about 1977. These can have superior performance to SAW counterparts in some applications. SBAW devices involve signal processing of acoustic bulk waves that are constrained to propagate close to the piezoelectric substrate surface. As listed in Table 2, SSBW resonators offer superior performance in some stable oscillators requiring higher power levels and/or reduced sensitivity to surface contamination and defects.

Manuscript received December 9, 1988; revised April 27, 1989. This work was supported in part by the National Sciences & Engineering Research Council of Canada.

The author is with the Department of Electrical and Computer Engineering, McMaster University, Hamilton, Ontario L8S 4L7, Canada.

IEEE Log Number 8929588.

0018-9219/89/1000-1453$01.00 © 1989 IEEE

Table 1 Representative Applications of SAW Devices

Device	Applications
Medium loss SAW filter, (nondispersive):	IF filtering. Clock recovery. Nyquist filters. MSK modulation.
SAW delay line:	Path length equalizers. Altimeters. Pressure and temperature sensors. Tunable oscillators. Recirculating storage.
Fixed-tap delay line:	Pulse compression radar. Barker and quadraphase coding. Radar return simulation.
Programmable transversal filter:	Adaptive filtering for spread spectrum. Matched filtering. Channel equalization. Radar simulator.
SAW Comb filter:	Multiplexers. Multimode oscillators. Counters.
Low-loss SAW filter:	VHF/UHF front-end filtering. Mobile and cellular radio. Antenna duplexer.
SAW resonator:	Precision filters and fixed oscillators.
SAW chirp filter:	Pulse compression radar. Variable delay lines and multipath cancellation. Real-time Fourier-transform processors. Wide-band linear-phase filters. Reflective array compressor with large TB product.
Three- and four-port SAW convolver:	Matched filtering in spread spectrum. Long-code correlation. Radar. Packet radio.
Acoustic charge transport on GaAs:	High-speed sampling. Wide-band pn-code correlator. Programmable filtering.
Other SAW devices on GaAs:	Tunable delay lines and resonators. Programmable filters and correlators.
SAW-based optoelectronic devices:	Bragg modulators. Spectrum analyzers. Wide-band convolvers and correlators. Monolithic integration on GaAs.
Multilayered SAW devices:	Rugged resonators and filters. Monolithic SAW convolvers and correlators. Sensors.

Table 2 Some Current Applications of SBAW Devices

SBAW Type	Applications
SSBW devices:	Mid-loss filtering with reduced sensitivity to surface contamination. Operating frequencies up to about 60-percent higher than SAW-based counterparts.
STW devices:	Low-loss filters. Resonators with higher-power capability than SAW. Stable oscillators.

Moreover, SBAW filters can be configured with center frequencies up to about 60-percent higher than with SAW devices using the same piezoelectric substrates and transducer geometries.

Many features of SAW-device technology can be readily transferred to SBAW implementation, since they involve the same microelectronic fabrication and production processes and may use the same piezoelectric materials. Some SBAW devices can be visually indistinguishable from their SAW counterparts, differing only in the piezoelectric crystal orientations employed.

Mechanical wave propagation in SBAW devices is often referred to as surface skimming bulk waves (SSBWs) when only input and output IDT structures are involved. In SBAW resonators incorporating energy-trapping gratings, the wave motion is usually termed a surface transverse wave (STW) one. Table 2 lists signal-processing applications of both of these SBAW-device types.

B. Aim of this Paper

In this paper, the salient features of significant SAW and SSBW devices are reviewed in terms of their device parameters and performance. It is assumed that the reader has some knowledge of SAW device principles. For the SAW-device review, emphasis is given to developments over the past 10 years. Interested readers seeking more background material are referred to a number of textbooks dealing with various aspects and treatments of this subject [8]–[20]. Early key papers on SAW devices are to be found in [21]–[23]. Also, other review papers deal with SAW filters [24], components for electronic warfare receivers [25], SAW-device applications [26]–[29], SAW resonators [30]–[32], SAW materials [33], SAW waveguides [34], SAW waves and acoustoelectric interactions [35], [36], SAW reflective array structures [37], acoustooptic Bragg modulators for integrated optic communications [38], SAW-based fixed and adaptive filtering on GaAs [39], hybrid programmable transversal filters [40], and SAW-based acoustic charge transport (ACT) processes and structures on GaAs [41]. Principles of SBAW propagation and devices are contained in [42] and [43]. A sensor classification scheme is presented in [44]. The use of SAW convolvers in spread-spectrum communications is reviewed in [45]–[47], with wide-band packet radio emphasized in [48]. Specifics of SAW Fourier transform processors for interference rejection in spread-spectrum communications, adaptive filtering, real-time spectrum, and cepstrum analysis for radar and sonar are in [19], [49], and [50]. SAW and SBAW propagation in gallium arsenide are examined in [51] and [52].

Open-literature publications on SAW and SBAW devices are largely documented in a) IEEE TRANSACTIONS ON ULTRASONICS, FERROELECTRONICS, AND FREQUENCY CONTROL and its precedessor IEEE TRANSACTIONS ON SONICSAND ULTRASONICS, b) annual *IEEE Ultrasonics Symposium Proceedings*, c) PROCEEDINGS OF THE IEEE, and d) *Proceedings of the Annual Frequency Control Symposium*. In view of the mass of literature on these subjects to date, references in this paper mainly relate to the first three sources.

II. SAW CRYSTALS AND LAYERED STRUCTURES

A. Representative SAW-Filter Specifications

Key parameters for nondispersive SAW bandpass filters, with typical commercial specifications, are shown in Table 3. The choice of piezoelectric substrate is basic to attainment of such specifications, involving tradeoffs between insertion loss, filter fractional bandwidth, temperature stability, and shape factor (SF), where SF = $\Delta f_r/\Delta f$ such that Δf = bandwidth at 1-dB points Δf_r = ultimate rejection bandwidth (and SF = 1 is ideal). Figure 1 shows the response of a precision commercial SAW filter for 70-MHz IF operation.

Table 3 Typical Commercial Specifications for Nondispersive SAW Filters

Filter Parameter	Specifications
Center frequency:	10 MHz to 2 GHz
Insertion loss:	<3 dB to >30 dB
Fractional bandwidth Δf @ 1 dB:	0.06% to 40%
Transition bandwidth:	0.35 MHz to 2 MHz
Shape Factor:	<1.1 to >1.5
Passband Amplitude ripple:	± 0.3 dB
Peak phase deviation:	± 3°
Close-in sidelobe level:	30 dB to 60 dB

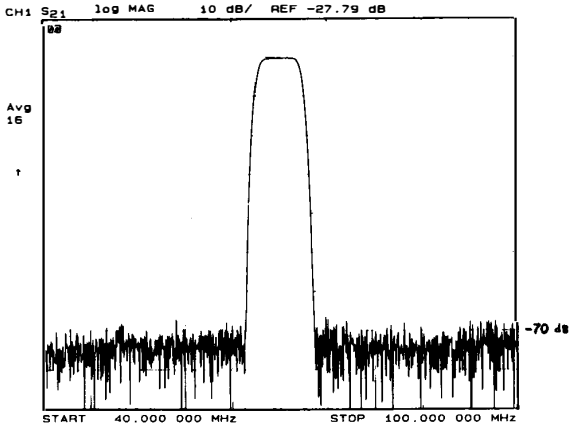

Fig. 1. Frequency response of a precision SAW filter with 70-dB out-of-band rejection. Horizontal scale: 40–100 MHz; vertical scale: 10 dB/div. (Courtesy of Crystal Technology, Inc., Palo Alto, CA.)

B. Single-Crystal Substrates for SAW IDTs

Figure 2(a) shows an elementary SAW filter employing input and output interdigital transducers (IDTs) on a single-crystal piezoelectric substrate, while Fig. 2(b) gives an equivalent circuit for each IDT in terms of radiation conductance G_a, radiation susceptance B_a, and transducer capacitance C_t. The filter frequency response is dictated by the electrode geometry of the voltage-excited input and output IDTs for launching and detecting the SAW motion. Insertion loss (IL) depends on the degree of match between IDT impedances and load/source counterparts.

Single-crystal *Y*-cut *Z*-propagating (*Y*-*Z*) lithium niobate

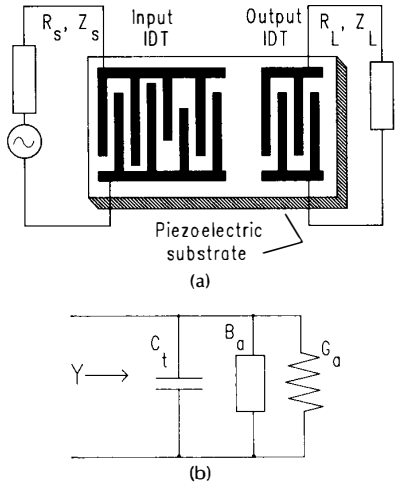

Fig. 2. (a) Elementary SAW filter with input/output IDTs on single-crystal piezoelectric substrate. (b) Equivalent circuit for an IDT based on crossed-field model.

($LiNbO_3$) and ST-X quartz piezoelectric crystal substrates were initially the mainstay of SAW bandpass filter design. Lithium niobate, with relatively large electromechanical coupling coefficient K^2 (normally expressed as a percentage) is employed in wide-band filters where temperature sensitivity is not crucial. Quartz, with a first-order zero-temperature coefficient of delay (TCD) around room temperature, is used in narrow-band designs (<5 percent) requiring temperature stability. Table 4 lists important filter-design parameters for these piezoelectrics, together with others in use or under development in aiming for large values of SAW velocity v, large K^2, and/or low TCD. These include piezoelectric thin-film composites as well as single-crystal substrates.

In the mass-production of low-cost SAW TV-IF filters in Japan, most are fabricated on a) single-crystal *X*-112° *Y* lithium tantalate (i.e., X-cut $LiTaO_3$ with propagation 112° from *Y* towards *Z* (see [54]), followed by b) single-crystal 128° *Y*-*X* $LiNbO_3$ (i.e., 128° rotated-*Y* cut, with *X*-propagation), c) thin-film zinc oxide (ZnO) sputtered on glass for high-impedance devices, and d) various piezoelectric ceramics [5]. Also in Japan, some narrow-band filters for receiver front-ends in paging systems at 280 MHz employ SAW mul-

Table 4 Some Piezoelectrics for SAW Substrates and Layered Structures

Substrate	SAW Velocity v (m/s)	K^2 (%)	1st-Order TCD Mag. (ppm/°C)	Comments
ST-quartz:	3158	0.14	0	Up to 25 cm long, Ref. [26].
Y-Z $LiNbO_3$:	3488	4.5	94	Up to 25 cm long
128°rotated-Y X $LiNbO_3$:	3992	5.3	75	Up to 25 cm long
SiO_2 on 128°-Y X $LiNbO_3$:	≃3800?	≃8.0	≃0	Large K^2, Ref. [63]
$Bi_{12}GeO_{20}$:	1681	1.4	120	(110)-cut, ⟨001⟩-propagation
GaAs:	<2841	<0.06	35	For (100)-cut with ⟨110⟩ propagation.
Rotated-Y cut Z'-prop. $LiTaO_3$:	3254	0.72	35	Minimum diffraction cut, Ref. [53]
X-cut 112° Y-prop $LiTaO_3$:	3288	0.6	18	Low bulk wave emission
X-Z $Li_2B_4O_7$:	3562	≃1	6.2	Can dissolve in water and acids, Ref. [55]
ZnO/AlN/Glass:	5840	4.3	21	Uses Sezawa mode of Rayleigh wave, Ref. [58].

timode coupling structures on X-112°Y $LiTaO_3$ or on X-cut Z-propagating lithium tetraborate ($Li_2B_4O_7$). Lithium tetraborate can be troublesome to work with, as it can be dissolved in water or acid. It has four acoustic modes of propagation: one SAW and three bulk-wave components. SAW delay lines with 10-dB insertion loss at 219 MHz have been reported, with TCD ≃ 6 ppm/°C, a good contender to replace quartz in narrow-band applications [55]. Berlinite (α-$AlPO_4$) single crystals have also been under investigation as an alternative to quartz in microwave acoustic applications [64], [65].

While a variety of crystal cuts exists for SAW propagation on gallium arsenide (GaAs) [39], [52], the listing in Table 4 is for the (100)-cut with ⟨110⟩-propagation, for maximum K^2 and compatibility with other GaAs-based integrated-circuit technology [52].

C. Layered Structures for SAW Propagation

Among the layered structures employing thin- or thick-film piezoelectrics, the composite ZnO/AlN/glass can yield K^2 = 4.37 percent, TCD = 21 ppm/°C, and v = 5840 m/s [58]. In a device operating with less than 10-dB insertion loss at 97 MHz, the above results were simultaneously obtained using a dispersion-thickness (kH) parameter kH = 1.05 for the ZnO and kH = 1.5 for AlN. [58] Sputtered piezoelectric zinc oxide (ZnO) films are polycrystalline with c-axis orientation having a reported standard deviation of the c-axis distribution, around the substrate normal, of less than 2 percent [56], [57]. In addition, the aluminum nitride (AlN) piezoelectric thin film is a polycrystalline sputtered one, with the c-axis normal to the substrate surface [58].

AlN on glass may be used as an inexpensive substitute for sapphire and ceramic substrates, while providing high acoustic velocity. Wave propagation in this composite involves the Sezawa (or leaky) surface wave, which is the first higher order mode of the Rayleigh wave.

SAW delay lines operating above 1 GHz have also been reported using *epitaxial* AlN films on sapphire (i.e., aluminum oxide Al_2O_3) as well as on silicon (Si) substrates. A TCD ≃ 0 value was obtained for the AlN/Al_2O_3 combination [59]. Potential use of this last structure includes a SAW correlator in a one-chip radio-frequency integrated circuit for a spread-spectrum transceiver [59].

Epitaxial single crystal ZnO films have also been employed in the structure (0001)ZnO/SiO_2/(111)Si, using fused-quartz (SiO_2), where the SAW velocity could be selected from 2700–4500 m/s by changing the ZnO and/or SiO_2 film thicknesses [60]. Composite structures of the ZnO/Si type are of interest for signal processing using monolithic SAW convolvers on silicon [61].

ZnO thin-film SAW video intermediate frequency (VIF) filters for color TV sets have been in production for several years. In these devices, one set of unapodized Al input/output IDTs is placed between a borosilicate glass substrate and a thin polycrystalline ZnO film deposited by RF sputtering [60]. Additional Al thin-film counter electrodes are deposited on top of the ZnO, as shown in Fig. 3(a), to allow for apodization weighting. Figure 3(b) outlines the structure of such a commercial VIF filter using two parallel-connected output IDTs for low-loss operation around picture and sound carriers (Japan) of 58.75 MHz and 54.25 MHz, respectively, without a preamplifier. The input IDT is staggered to provide the required nonlinear phase and TV adjacent channel nulls for picture and sound [60].

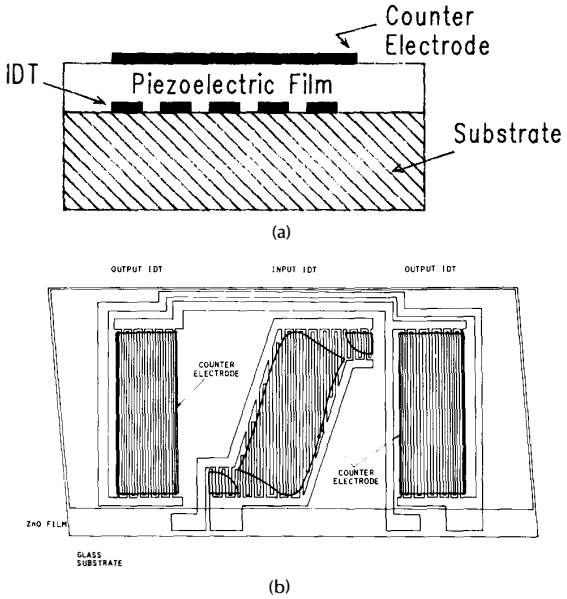

Fig. 3. (a) Placement of counter electrodes in thin-film SAW device. (b) Geometry of low-loss ZnO thin-film SAW VIF filter using counter electrodes. (Reprinted with permission from Yamazaki, Mitsuyu, and Wasa, see [60].)

SAW structures have also been fabricated to yield low TCD by overlaying a thin SiO_2 layer with negative TCD on to a piezoelectric substrate with positive TCD such as $LiNbO_3$ or $LiTaO_3$ [62], [63]. Using a thick RF sputtered film (h/λ = 0.310) of SiO_2 on 128°Y-X $LiNbO_3$, a TCD ≃ 0 was obtained, together with a high value of K^2 = 0.08 [63].

III. SAW Transducers and Filter Modeling

A. The Interdigital Transducer (IDT) and SAW Excitation

As sketched in Fig. 2(a), the basic SAW filter incorporates thin-film voltage-excited input and output IDTs deposited on the mirror-like surface of a piezoelectric single crystal substrate. The time-varying electric fields between adjacent electrodes in the input IDT convert electrical signals into mechanical (and bidirectional) surface acoustic wave (SAW) motion. The converse takes place at the output IDT. The penetration of the SAW into the piezoelectric is about one acoustic wavelength λ (e.g., $\simeq 10 \times 10^{-6}$ m in Y-Z lithium niobate at 300 MHz), hence the requirement for a high-quality surface finish.

The desired filtering function is achieved by the apodization (i.e., finger overlap) applied to input and/or output IDTs. In the input IDT, the amplitude and phase of individual SAW emissions are dictated by finger overlap and polarity. If applied in the receiver IDT, apodization governs the relative amplitude and phase of voltages induced in each finger pair, and the resultant voltage at the summing bus. In the example of Fig. 2(a) for an elemental SAW bandpass filter with (nominal) linear phase response, the normal spacing between IDT fingers of alternating polarity is $\lambda_0/2$ at filter center frequency $f_0 = v/\lambda_0$. If the frequency response of the input IDT in Fig. 2(a) is $H_1(\omega)$ and that of the output

one is $H_2(\omega)$, the overall response $H(\omega)$ will be given by $H(\omega) = H_1(\omega) \cdot H_2(\omega)\, e^{-j\beta d}$, where $\beta = 2\pi/\lambda$ = phase constant and d = distance between IDT phase centers. The inherent delay time τ is $\tau = d/v$.

The overall device insertion loss (IL) is dictated by mismatch loss between IDTs and respective source/load impedance, as well as by second-order effects considered below. For given IDT geometries, the degree of mismatch loss will be dependent on the electromechanical coupling coefficient K^2 of the piezoelectric substrate. Moreover, bidirectionality of SAW emissions results in minimum insertion loss of 3 dB per IDT or 6-dB minimum overall.

B. Other Techniques for SAW Generation or Detection

While transducers employed in SAW-filter design are IDTs of the voltage-excited type described above, other transducer types find use in specialized applications. Current-excited electromagnetic-acoustic transducers (EMATs), using meander lines for SAW excitation [66], have been used for noncontacting inspection of metallic surfaces [67], as well as for the measurement of the vertical and horizontal displacements of surface waves [68].

SAW waves can also be generated by pulsed laser excitation of a material surface. This technique finds application to materials inspection of cracks and slots using, for example, a Q-switched Nd:YAG source for measuring defect depths in the range 0.1–5 mm [69]. Laser excitation of SAW can also be applied to high-resolution Rayleigh velocity measurements on SAW waves [70], [71], as well as probing SAW generation and detection by IDTs [72]. This laser technique has also been applied to probing SAW waveguide convolvers, to measure the propagation attenuation of specific acoustic modes [73], [74].

C. Second-Order Effects

The performance of a SAW filter can be corrupted to an unacceptable degree by any one of a number of second-order effects, unless these are minimized or compensated for. These include the following.

1) *Electromagnetic (EM) feedthrough* between IDTs causing in-band and out-of-band amplitude and phase ripple. The level of EM feedthrough generally increases with increasing frequency and can be most troublesome in UHF and gigahertz SAW filters, requiring exacting packaging and avoidance of ground loops. 2) *Triple-transit-interference* (TTI) associated with multiple regenerative and/or nonregenerative SAW reflections between bidirectional IDTs, which can cause excessive in-band ripple when the insertion loss is low. Significant reduction of TTI is achieved by mismatching source and/or load impedances to their IDTs, with the penalty of increased insertion loss. 3) *Mass-loading* by the metal IDT fingers causes SAW velocity changes which can alter the desired response. 4) *Bulk waves* will radiate from an excited IDT to some extent, in addition to the SAW emissions. These will corrupt the passband response and also reduce out-of-band rejection. Since the bulk-wave component velocities are higher than for SAW, passband distortion will tend to be most pronounced at the high-frequency band edge, particularly in large-bandwidth (BW) filters (i.e., BW $> \simeq 25$ percent). In Y-Z lithium niobate, the amount of bulk-wave generation relative to SAW becomes large when the number of IDT finger pairs $N \leq \simeq 5$, corresponding to filter 4-dB bandwidth $BW_4 = 100/N \geq 20$ percent [75]. 5) *Circuit factor loading* results from finite source and load impedances. Since the input and output impedances of a SAW filter are frequency-dependent parameters (see Fig. 2(b)), voltages developed across input and output IDTs are frequency-dependent unless compensated for. 6) *Diffraction* occurs in SAW IDTs in the same manner as in optical systems, with Fresnel (near-field) and Fraunhofer (far-field) regions. Input and output IDTs should be in each other's Fresnel zone, for minimum diffraction. Its principal effect will be to increase filter transition band and shape factor, as well as to reduce the level of close-in sidelobe suppression. Diffraction is a reciprocal effect, and cannot be circumvented by reversing the input/output stages. 7) *Harmonics* can be generated by excited IDTs, in addition to the fundamental. This may be a desirable or an undesirable feature, depending on the application. Harmonic frequencies and levels will depend on the width-space ratio of an IDT finger (i.e., the metallization ratio η) and on the IDT geometry employed [76]–[82].

D. IDT Structures

In the basic IDT of Fig. 4(a), employing "single-electrode" geometry and uniform finger spacing, the IDT electrode periodicity is *normally* such that the desired filter center frequency $f_0 = f_s$, where $f_0 = v/\lambda_0$, λ_0 = acoustic wavelength, and f_s is the IDT synchronous frequency. The finger sampling frequency f_d is $f_d = 2f_s$ for single electrodes alternating in excitation polarity. In the "split-electrode" IDT of Fig. 4(b), $f_0 = f_s$ still, while the finger sampling frequency is now $f_d = 4f_s$. The split-electrode geometry of Fig. 4(b) is usually favored over the single-electrode one in "normal" linear phase filter designs where $f_0 = f_s$. The split electrodes serve to negate the spurious response due to finger reflections at center frequency. As well, the higher sampling frequency $4f_s$ allows for designing passbands with nonsymmetric amplitude and/or nonlinear phase response [83]. Moreover, the split-electrode finger lengths can be adjusted to pre-distort the filter response for diffraction compensation [84].

E. Modeling of SAW Filters with Bidirectional IDTs

Many models have been developed to relate the frequency and impulse response of linear phase IDTs of Fig. 4(a) and (b), while accounting for the numerous second-order effects that corrupt the ideal performance. Three models introduced at an early date are the *delta-function model* [85], [86], the *impulse response model* [87], and the *crossed-field model* [88]–[90]. The delta function neglects any second-order effects in modeling the frequency response $H(\omega)$ of each IDT in Fig. 2 as a transversal filter, where

$$H(\omega) = \sum_{n=1}^{N} A_n e^{-j\omega T_n} \tag{1}$$

where $T_n = nT$ for uniform electrode finger spacing, and $A = a_n e^{j\Phi_n}$ is the (relative) complex SAW potential associated with each excited finger. The overall filter response is then (ideally) $H_{in}(\omega)H_{out}(\omega)\, e^{-j\beta d}$, in terms of input and output IDT responses $H_{in}(\omega)$ and $H_{out}(\omega)$, as well as the phase shift βd between phase centers of IDTs separated by distance d.

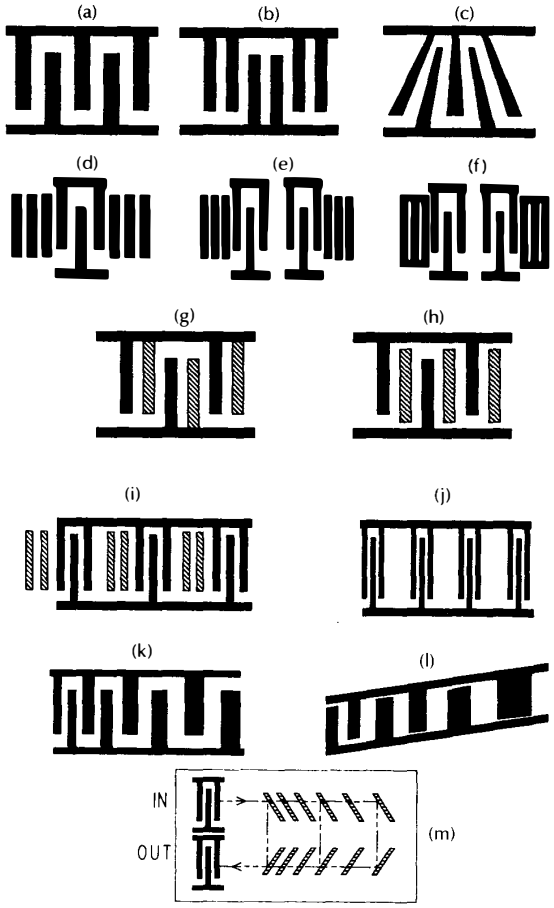

Fig. 4. SAW IDTs and structures for (a) single-electrode IDT geometry, (b) split-electrode IDT, (c) slanted/curved IDT on collimating substrate—shown with exaggerated tilt, (d) one-port resonator, (e) two-port resonator with open-circuited reflection-grating elements, (f) two-port resonator with short-circuited reflection-grating elements, (g) double-metallization SPUDT, (h) floating-electrode SPUDT, (i) Lewis-type SPUDT, (j) "conventional" comb filter, (k) in-line chirp IDT, (l) chirp IDT for slanted-array compressor (SAC), and (m) geometry of a reflective array compressor (RAC) using etched-groove reflectors.

Restrictions placed on the apodization of both IDTs are apparent with this model.

The impulse response model yields additional information on input and output impedance levels, as well as on the frequency sensitivity of individual electrodes. This model employs the Fourier-transform relations

$$H(\omega) = \int_{-\infty}^{+\infty} h(t)\, e^{-j2\pi ft} dt \tag{2}$$

$$h(t) = \int_{-\infty}^{+\infty} H(\omega)\, e^{j2\pi ft} df \tag{3}$$

for a linear system, with a one-to-one correspondence between $H(\omega)$ and $h(t)$, where $h(t)$ is the impulse response. This is most useful in SAW-filter design, since the finger overlap pattern (apodization) of an IDT is a spatially-sampled approximation to its impulse response. The accuracy will increase with the finite number of IDT fingers employed within the finite-substrate length.

Many network analyzers are now configured to display both frequency response and impulse response, where the latter is computed by applying a discrete Fourier transform to the measured frequency-response data. Observation of the impulse response of a SAW device is often essential in separating and identifying levels of second-order effects due to EM feedthrough, TTI, and other spurious SAW and bulk-wave reflections. In a different instrumentation approach, the frequency-response magnitude can be obtained from the impulse response without numerical processing, for direct display on a spectrum analyzer [91].

The crossed-field model also yields information on impedance levels. With sufficient modeling, it can also account for harmonic responses and TTI. In this model, each IDT is considered as a three-port structure with two acoustic ports and one electrical port, with a 3×3 admittance matrix $\{Y\}$ relating the acoustic and electrical parameters for each three-port.

Alternative approaches to modeling the IDT include the use of a scattering matrix $\{S\}$ [92], as well as a transmission matrix $\{T\}$ [93], [94]. The transmission matrix can also be used to model the frequency response of SAW filters using parallel-connected banks of bidirectional IDTs (known as interdigitated interdigital transducers (IIDTs)) for low insertion-loss applications such as receiver front-end filtering [95].

F. Computer-Aided Modeling

Computer-aided design (CAD) techniques are readily applicable to SAW-filter design on single-crystal piezoelectric substrates. These can allow interactive analysis and modeling of: 1) the frequency-dependent acoustic conductance G_a and Hilbert-transform susceptance B_a in Fig. 2(b); 2) magnitude, phase, and group delay; 3) TTI and EM interference; 4) input/output impedances; and 5) impulse response [96]. In addition, a variety of window functions can be applied to optimize passband response, including those of the Hamming, Blackman, or Kaiser-Bessel-type [97], [98]. Some CAD programs may also be specifically applied to withdrawal-weighted IDTs [99] with sidelobe suppression of up to about 70 dB in narrow-band filters (BW $< \simeq 1$ percent) [100]–[102], where the use of a multistrip coupler (MSC) [103], [104] is undesirable.

A variety of linear-phase SAW-filter responses can also be obtained using CAD techniques incorporating the Remez exchange algorithm; originally applied to optimum linear-phase *digital filters*. These include SAW bandpass, bandstop, and amplitude-weighted equalizer filters, as well as multiband filters with up to 10 passbands implemented within one IDT [105]. Also, this Remez technique allows the user to set the IDT synchronism frequency f_s outside the pass band. An appropriate choice of $f_s \neq f_0$ then enables single-finger IDTs to be used, without finger reflections at midband [105].

G. Predicting Bulk-Wave Interference

Rigorous modeling may be applied to predict spurious bulk-wave responses in apodized IDTs. One approach uses Green's function formalism to relate piezoelectric surface potential and charge distributions over all electrodes in the

excited IDT [13], [106], [107]. In another technique applied to 128° *Y-X* $LiNbO_3$, each mode of bulk-wave transport is delineated in both the time and frequency domain [108].

H. Diffraction Analysis and Compensation

As noted above, the effect of diffraction on the response of a SAW bandpass filter can be most pronounced in the transition and stop bands. The simplest approach to minimizing this diffraction, of course, is to use IDTs with very wide acoustic apertures [109]. Where this is not feasible, diffraction compensation requires a knowledge of the SAW beam profile, which is dependent on the variation of SAW velocity v with propagation direction. Fast computations are required for efficient design algorithms.

Diffraction compensation has been extensively applied to single-crystal ST-X quartz, whose slowness surface about the pure-mode SAW propagation axis is approximated by a parabola. More general nonparabolic slowness surfaces, such as for *Y-Z* lithium niobate, require a full angular spectrum representation to calculate the effect of diffraction [84], [110]–[112]. The computation time for this can become excessive. One fast method for calculating SAW diffraction in anisotropic substrates uses an asymptotic expansion of the diffraction integral, which is accurate in the very near-field region. This technique increases the computation speed by a factor of at least 25 over those for direct numerical integration of the diffraction integral [113], [114].

Magnitude and phase compensation for diffraction are accomplished by adjusting the individual finger-pair overlaps in the split-electrode IDT of Fig. 4(b), together with the relative length of elements in each finger pair [84]. With such techniques, improvements in sidelobe suppression in the order of 15 dB can be attained [114].

I. Modeling the Acoustoelectric Field in Layered Structures

The above modeling discussions have tacitly applied to SAW devices on single, thick, piezoelectric substrates. Other models have been developed for layered structures propagating the Rayleigh (SAW) wave; and higher order acoustic modes such as the Sezawa wave. IDT static capacitance in multilayered devices can be computed using a transmission-line approach, in conjunction with an equivalence to Poisson's equation for Green's function [115]. Modelling has also been applied to the acoustoelectric interaction between surface acoustic waves and a semiconductor in the presence of a layer with different carrier concentration on the semiconductor surface [116].

Applications include multi-layer thin-film SAW devices on glass, Si, GaAs, or sapphire substrates. One approach applied to a three-layer structure of ZnO and AlN thin films on glass employs the same constitutive equations used to derive the Rayleigh wave in a single medium [58], [117]. Another ZnO thin-film model takes into account the crystal grain-random orientation as well as the lattice distortion [118].

An efficient iterative computational technique has also been applied to determine the acoustoelectric field of configurations where the IDT may be bounded on either side by an arbitrary number of layers. This method is limited to materials of hexagonal symmetry, with the axis of six-fold symmetry parallel to the IDT electrodes [119].

J. Modeling Wide-band Linear-Phase Filters and Delay Lines

Linear-phase SAW filters with bandwidths of up to 50 percent or more have been implemented on $LiNbO_3$ using slanted- or curved-finger IDTs as sketched in Fig. 4(c). Operation relies on the autocollimation properties of $LiNbO_3$ for finger tilt angles up to about ±7° about a normal to the SAW propagation axis. Delta function or generalized impulse response modeling may be applied to obtain the transfer function. Differing input/output IDT geometries can be employed to reduce passband ripple [120]–[122].

IV. SAW Resonators

A. Resonator Specifications

SAW resonators employing reflection gratings [123], [124] are employed for precision filtering and oscillator applications. High-Q SAW-resonator oscillators are now the preferred design for precision frequency-control application in the frequency range 200 MHz to 1 GHz, involving spectrum analyzers, frequency synthesizers, as well as carrier-noise test sets [125], [126]. Noise floors of −176 dBc/Hz have been reported for precision SAW-resonator oscillators [127]. The reflection gratings, comprised of several-hundred periodic and weakly-reflecting elements, provide high reflectivity over narrow stop bands and allow for operation with insertion-loss capability of less than 6 dB. Size restrictions normally limit their operation to above 100 MHz. Q-factors attainable (Q = 1/BW), ranging from ≃80 000 at 100 MHz to 3000–10 000 at 1 GHz compare favorably with BAW counterparts [129]. For single, thick, piezoelectric substrates, SAW resonators on ST-quartz offer excellent temperature stability with zero linear TCD near 25°C and a quadratic coefficient corresponding to a drift of ± 15 ppm over 0° to 55°C. While aging drifts of less than 0.1 ppm are attainable, typical SAW-resonator aging rates are between 1 and 10 ppm/year [132]. Recent SAW-resonator designs on quartz have reported Q = 2000 for a 2.6-GHz resonator, with insertion loss less than 11 dB [128].

Various loss mechanisms limit the attainable resonator Q. These include SAW to BAW mode-conversion in the gratings [130], resistive loss in the electrodes, and viscous damping in the substrate. Attenuation due to viscous damping increases as the square of the frequency. It also increases at low frequencies due to increased transmission through the finite-length gratings [130]. In addition, power-handling capabilities of SAW resonators are limited to a maximum of about 15–20 dBm. Excessive SAW power levels lead to frequency shifts of the resonator response and/or destructive failure due to migration of the IDT metallization by violent surface vibrations.

B. Resonator Geometries and Modes

Figure 4(d), (e), and (f) illustrate transducer geometries for one-port and two-port resonators. While the one-port structures can be employed for direct replacement of some BAW crystal resonators operating above 50 MHz in overtone modes [132], the two-port structures provide more design versatility [131]. Figure 5 shows the frequency response of a precision two-port SAW resonator operating at 1 GHz.

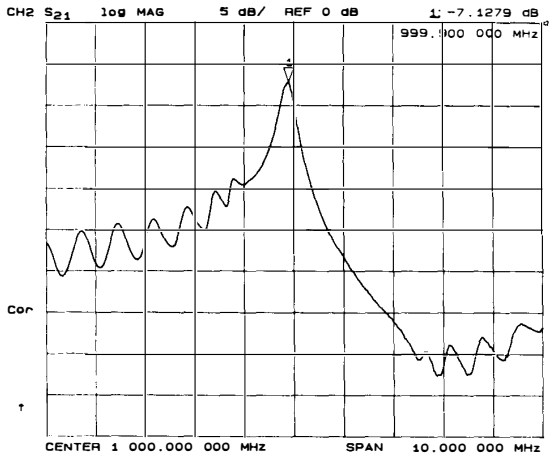

Fig. 5. Transmission response of a precision 1-GHz two-port SAW resonator. Horizontal scale: 1-GHz center frequency with 10-MHz span; Vertical scale: 5 dB/div; Marker at 999.9 MHz. (Courtesy of Hewlett Packard Laboratories, Palo Alto, CA.)

Centers of SAW reflections in periodic reflection gratings are at the edges of grating element. Centers of reflection in excited IDT on the other hand are mid-finger positions. This gives a positioning difference of $\lambda_0/8$ at center frequency for metallization ratio $\eta = 0.5$ [133]-[135]. (This acoustic wavelength difference is also to be found in some natural orientations of IDTs on quartz and $LiNbO_3$ [136].) Optimum resonator response requires correct positioning of gratings with respect to IDTs. This is dictated by the magnitude and phase of the grating reflection coefficient, which is a function of the type of grating (open strips, shorted strips, grooves, etc.) as well as the substrate employed [8], [93], [137], [138].

SAW reflections from IDTs can be detrimental to SAW resonator performance. With quartz substrates, this effect has been reduced by using recessed aluminum IDTs, yielding Q values over 3200 at 1 GHz [32]. In the grating reflector, scattering of the SAW into bulk waves will result in increased insertion loss, with a 3.5-dB loss demonstrated for normal incidence grating with 200 grooves and $h/\lambda \simeq 2.1$ percent [130].

C. SAW Narrow-Band Resonator-Filters

In two-port SAW resonators, single-mode operation occurs when the resonant spacing between IDTs is reduced to support only one mode within the width of the grating stop band. Multimode operation can be attained by increasing the resonant spacing between IDTs [137]. This capability has applied to the design of narrow-band SAW filters (BW $\simeq$ 1 percent) on lithium niobate, using a staggered resonator structure [139]. Staggered two-port SAW resonators have also been employed for harmonic operation, with a $Q = 2213$ demonstrated for such a structure operating in the fifth-harmonic mode [140].

Narrow-band SAW filters using coupled SAW resonators have also been extensively examined for insertion loss less than 6 dB and $500 \leq Q \leq 50\,000$ [93], [141], [142]. Resonator interconnections can include transducer, multistrip, waveguide, folded-acoustic, or unidirectional acoustic coupling. Gratings have been fabricated using shallow grooves, metal strips, dots, or ion-implanted strips to achieve the desired impedance discontinuity $\Delta Z/Z$ [141]. SAW resonator filters with up to size poles have been designed [143]. As an example of this technique, a two-pole design at 150 MHz exhibited 2-dB insertion loss and 70-dB rejection at $\pm$ 4 MHz [144]. Two-pole resonator filters on X-cut 112° Y-propagation $LiTaO_3$, 128° Y-cut $LiNbO_3$, and quartz are now in widespread use in Japan for paging systems in the 280-MHz band [5]. Figure 6 illustrates the compact packaging of a commercial 5 mm × 3 mm four-cavity SAW-resonator filter, chip-ribbon bonded to a ceramic base. Substrates are 0.5-mm thick, 50-mm diameter, 38.4° Y-rotated quartz with SAW propagation along the X-axis, chosen to give zero TCD at 35°C [125].

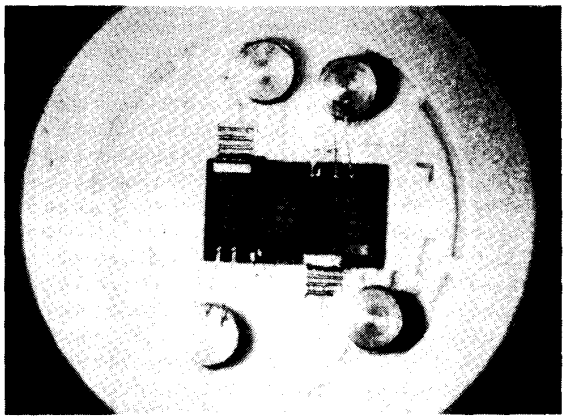

Fig. 6. Photograph of a 3 × 5-mm four-cavity SAW resonator chip ribbon-bonded to ceramic base. (Reprinted with permission from Bray, see [125].)

D. Analytic Methods

Analytical approaches to the design of SAW resonators and narrow-band filters on single-crystal substrates include the use of the scattering matrix $\{S\}$ [145], cavity analysis [146], and coupling-of-modes (COM) analysis [93], [133]-[135]. One COM approach employing an unweighted 2 × 2 complex grating matrix $\{G\}$, in conjunction with a 3 × 3 transducer matrix $\{T\}$ and a transmission line matrix $\{D\}$ [93], is readily extendable to the design of low-loss single-phase unidirectional transducers (SPUDTs) [94].

Grating reflectors can also introduce undesirable transverse-mode responses [147]. These can be decreased or eliminated by use of tapered gratings [148], [149].

E. SAW Resonators Using Layered Structures

SAW resonators have also been fabricated with layered structures. For example, an $ZnO/SiO_2/Si$ layered resonator with the ZnO limited to the IDT regions, (and etched-groove gratings on either the SiO_2 or Si), yielded Q-values in excess of 20 000 at 115 MHz [150]. Resonators of this type can have temperature stabilities comparable to quartz. One-port SAW resonators are also in wide use that employ a leaky SAW on 36° Y-cut X-propagating $LiTaO_3$, for high K^2 with moderate temperature stability. In this structure, the grat-

ing pitch and IDT finger spacing are slightly different, with the aim of canceling bulk waves from gratings and IDTs. This design was established using a theoretical analysis of bulk-wave radiation from the grating reflector elements [151].

F. Notch Filters Using SAW Resonators

A two-port SAW resonator can be configured for either 0° or 180° phase shift at center frequency. By connecting a suitable shunt network across the 180° structure, highly-selective notch-filter action can be achieved. Designs have been reported yielding 40-dB rejection over BW = 0.035 percent at 200 MHz, with an insertion loss of 1.5 dB ± 1.5 dB from DC to 800 MHz [152].

V. Low-Loss SAW Filters

A. Low-Loss SAW-Filter Types

Low-loss SAW-filter design involves some design tradeoffs, regardless of the structure employed. These include one or more penalties in fabricational complexity, device size, matching networks, bandwidth, passband ripple, and sidelobe sidelobe suppression. Apart from the resonator-filters considered above, various other low-loss SAW filter designs include those with multistrip couplers [103], [104], three-phase IDTs [153], group-type IDTs [154], and interdigitated IDTs [95], [155].

In recent years, considerable interest has evolved in the design of low-loss SAW filters for VHF/UHF receiver front-end circuitry. Low-loss filters are required in these stages, since the signal-to-noise performance is degraded by the amount of filter insertion loss. This has led to a focusing of attention on the use of low-loss single-phase unidirectional transducers (SPUDTs) for filters with fractional bandwidths BW ≃ 1 to 5 percent. Some SPUDT geometries are outlined in Fig. 4(g), (h), and (i). Fractional bandwidths of up to 10 percent have also been reported, with a further tradeoff in insertion loss [156]. All of these exploit the λ/8 wavelength difference between the centers of transduction and reflection in an electrode of metallization ratio $\eta = 0.5$. Unlike bidirectional IDTs, the unidirectionality of the SPUDTs allows matching at both the electric and acoustic ports. Also, coupling-of-modes (COM) analysis can be readily applied to some SPUDT designs.

In the original SPUDT design [135] shown in Fig. 4(g), the λ/8 transduction difference parameter was obtained by using two separate metallizations of aluminum and gold. The same end result can be obtained by using aluminum electrodes of differing thickness. Use of a shadow-casting technique to achieve such a SPUDT filter yielded an insertion loss IL ≤ 2.8 dB in a UHF filter at 500 MHz on 128°*Y*-*X* $LiNbO_3$ [157]. This structure also exhibited a minimum insertion loss of 1.5 dB at 1 GHz, with a tradeoff in increased passband ripple [158].

The SPUDT of Fig. 4(h) with "floating" internal reflector electrodes comprised of open and shorted metal strips has been reported with insertion loss IL ≤ 2.3 dB and bandwidth BW ≃ 3 percent at 97 MHz on 128° *Y*-*X* $LiNbO_3$, with electrode pairs in input and output SPUDTs. Here, the λ/8 displacement electrode is obtained by judicious placement of the reflector electrodes [159], [160].

The SPUDT filter of Fig. 4(i) is composed of banks of short reflection gratings placed to give the λ/8 displacement relative to adjacent banks of IDT "rungs" [161]. This positioning is dependent on whether open or shorted grating strips are used, as well as on the piezoelectric substrate. Typically, each SPUDT has a total of 100 reflectors strips divided between 10 IDT rungs. Differing rung periodicities are employed in input and output SPUDTs. An insertion loss capability of IL ≤ 2.6 dB at 80 MHz has been reported for such structures on lithium niobate with BW = 1 to 1.5 percent [94].

B. Increasing Sidelobe Suppression in SPUDT Filters

A problem with unweighted SPUDT filters is that the close-in sidelobe suppression is usually only about 20 to 25 dB. This has been increased to 40 dB in the SPUDT of Fig. 4(i), however, by weighting the IDT rung apertures, with some tradeoff in insertion loss to IL = 4.9 dB [156]. Slanted SPUDTs have also been reported with fractional bandwidths up to 10 percent [156]. Moreover, close-in sidelobe suppression of 70 dB was attained using two cascaded and weighted SPUDTs, with overall insertion loss IL = 8.5 dB and fractional bandwidth BW = 1.5 percent as shown in Fig. 7 [162].

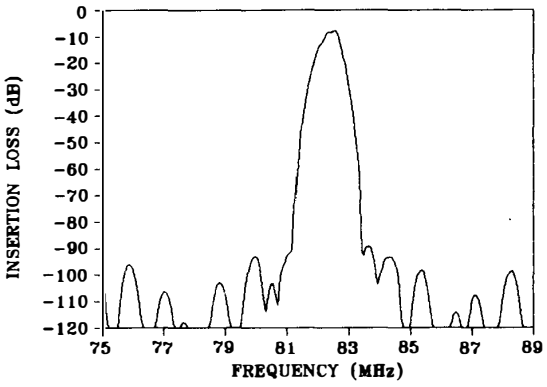

(a)

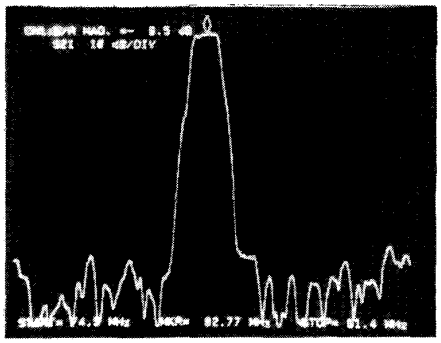

(b)

Fig. 7. (a) Predicted frequency response of low-loss cascaded SPUDT filter, using COM method. Horizontal scale: 75–89 MHz; vertical scale 10 dB/div. (b) Measured response over 75–91 MHz, with vertical scale 10 dB/div. Bandwidth 1.5%. Insertion loss 8.5 dB at 82.77-MHz marker. Sidelobe suppression 70 dB. (Reprinted with permission from Campbell and Saw, see [162]. Courtesy of *Electronics Letters*.)

VI. SAW Comb Filters and Multiplexers

A. Conventional SAW Comb Filters

Figure 4(j) shows one form of a "conventional" SAW comb filter involving a tapped delay-line structure with rungs of the same periodicity in equal input and output IDTs. Because of the small number of electrodes per rung required for broad-band operation, these filters have high insertion loss (e.g., 20 to 40 dB). The bandwidths BW_c of individual comb responses in this particular structure are $BW_c \simeq 0.72 f_0/R \cdot W$, while the number of comb modes M within the overall $(\sin X)/X$ amplitude envelope is $M \simeq (W/N) + 1$. In addition, the separation Δf_c between comb peaks is $\Delta f_c = f_0/W$, where W is the number of acoustic wavelengths at center frequency f_0, N is the number of finger pairs in each IDT rung, and R is the number of rungs in each IDT [8].

Such comb filters can find a variety of applications. For example, Hitachi has employed a set of four two-rung comb filters in a TV channel indicating system with frequency synthesizer. Each TV channel number is identified by counting the number of comb peaks after the local oscillator starts its sweep [163]. In another example, a SAW comb filter is used as the feedback element in a multimode SAW local oscillator for a frequency hopping radar [164]. One such oscillator, fabricated on ST-quartz, operated at center frequency $f_0 = 400$ MHz, with $R = 50$ rungs, rung spacing $W = 40\ \lambda_0$, and $N = 2$ finger pairs in each IDT. This gave $M = 26$ comb modes with a $Q \simeq \pi RW = 6280$ for each mode [164].

B. Low-Loss SAW Comb Filters

Wide-band low-loss comb filters have been reported, using the SPUDT filter of Fig. 4(i), but with identical IDTs in input and output. One such comb filter yielded a minimum insertion loss of 3.7 dB, together with a separation of 10 MHz between adjacent comb modes [165]. The wide-band capability is a consequence of the added signal-sampling introduced by the periodically-spaced reflection gratings, despite the fact that each grating has a narrow stop band [166].

C. SAW Multiplexer Techniques

SAW multiplexer action is readily achieved by using a broad-band input IDT of wide acoustic aperture to illuminate separate frequency-selective output IDTs, which may or may not be contiguous. Frequency measurements of narrow RF pulses require contiguous filter banks, which should be highly-selective in the frequency domain and distortionless in the time domain. One approach to this in an eight-channel design, yielding excellent performance in both domains, employed flat-exponential SAW filters on the minimal diffraction cut of lithium niobate. This yielded time-spurious suppression in excess of 44.5 dB, with low VSWR [167].

Another SAW multiplexer design employs hyperbolically-tapered input and output IDTs [121], [168]. The small-aperture output IDTs are positioned on either side of the single wide-aperture input IDT covering the total frequency band. In this way, a 14-channel multiplexer with a total bandwidth of 120 MHz (1 octave) centered at 180 MHz achieved 40-dB out-of-band rejection with insertion loss IL = 19 dB. When cascaded, these filters yielded 80-dB out-of-band rejection with IL ≃ 30 dB [168].

A quite different SAW multiplexer technique, employing staggered offset half-length multistrip couplers, was developed for a 16-channel SAW multiplexer for range-line resolution in frequency-modulated continuous-wave (FMCW) millimeter-wave radar. This was centered around an IF frequency of 85 MHz, as shown in Fig. 8. Channel separation

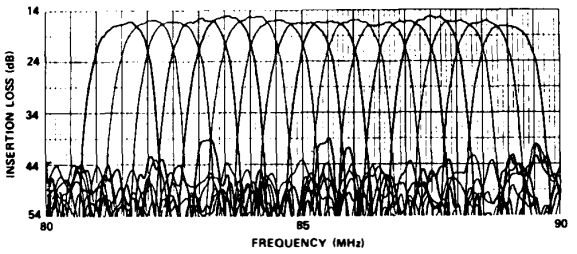

Fig. 8. Frequency response of 16-channel SAW-based multiplexer for FMCW millimeter-wave radar. Horizontal scale: 80–90 MHz; vertical scale: 10 dB/div. (Reprinted with permission from Solie and Wohlers, see ref. [169].)

was 0.5 MHz, with a 3-dB bandwidth of 1 MHz for each. Range-bin widths of about 0.1 to 0.5 percent of range could be realized with this technique [169].

VII. SAW Chirp Filters

A. SAW Chirp Filter Types

SAW dispersive chirp filters, designed for linear or nonlinear FM response, are integral components of pulse-compression radar systems. Linear FM chirps with quadratic phase response are commonly used for reduced sensitivity to Doppler shift, while nonlinear ones are employed to improve the S/N performance (0.5–1 dB) over the former. SAW linear FM chirp filters are also used to implement variable delay lines, real-time Fourier-transform processors for spectrum and cepstrum analysis, and real-time adaptive filters. Three types of chirp filter transducers are shown in Fig. 4(k), (l), and (m), while Table 5 illustrates typical SAW chirp filter parameters, and the all-important time-bandwidth (TB) product giving compression gain.

Table 5 Illustrative Saw Chirp Filter Parameters

Parameter	Specification
Center frequency:	10 MHz to 2 GHz
Bandwidth B:	up to ≃1.1 GHz
Time dispersion T:	10 ns to 150 μs
Time-Bandwidth (TB) product:	up to 10 000
Phase deviation from quadratic:	≤0.5°
Pulse-compression sidelobes:	40 dB
Insertion loss:	25 to 55 dB

Figure 4(k) shows an in-line dispersive transducer with metallized fingers. With this structure, finger reflections and TTI normally restrict the usable TB product to $TB < 1000$. While the slanted-array compressor (SAC) of Fig. 4(l) also has modest TB performance, it offers reduced degradation of response due to electrode reflections. The reflective array compressor (RAC) of Fig. 4(m) is employed for the highest TB requirements up to $TB = 10\,000$. This RAC type can employ up to about 6000 oblique etched groove reflectors in each track [37], [170], [171]. An alternative struc-

ture using a metal reflective dot array (RDA) provides simpler fabrication, while attaining TB products $TB = 1000$–2000 [172]. The RAC, RDA, and SAC allow for the use of a phase plate between input and output transducers, to correct for deviations from the quadratic phase response that would otherwise reduce both compressed-pulse sidelobes and resolution.

B. Losses in SAW Up-Chirp and Down-Chirp Filters

In principle, SAW up-chirp and down-chirp filters should have the same response characteristics, except for the change in dispersion slope. In practice, however, use of the down-chirp structure is preferred. This is due to several effects caused by electrode reflectivity. On high-coupling substrates, piezoelectric shorting dominates, causing changes in SAW velocity and acoustic impedance. Mass-loading dominates on low-coupling substrates, such as quartz. Electrode reflections increase the level of TTI in the chirp filter. In addition, and as with SPUDT IDTs, they introduce some degree of acoustic unidirectionality into the filter performance. A result of this is that the down-chirp filters can have lower insertion loss than their up-chirp counterparts [13], [173]. Moreover, up-chirp structures have a 33-percent bandwidth limitation imposed on their use by SAW conversion to bulk waves [173]. As a result, pulse-compression systems employing both SAW expander and compression filters often employ down-chirp filters in the transmitter (expander) and receiver (compressor) stages, in conjunction with spectral inversion [174].

C. Examples for Pulse-Compression Radar

Ion-beam etched RACs on $LiNbO_3$ were originally employed for air/ground pulse-compression radar and wider bandwidth systems, with typical dispersions of $T = 40\ \mu s$ and compressed-pulse width of 200 ns [175]. Improved temperature stability and sidelobe suppression can be obtained in the air/ground systems using an RDA on quartz [170], such as the four-bounce type [172]. Figure 9 is a photo of a commercial RAC on quartz for a radar application, with dispersion $T = 80\ \mu s$.

As an illustration of current SAC capability, a SAC was reported operating at $f_0 = 1400$ MHz, with bandwidth $B = 1100$ MHz, dispersion $T = 440$ ns, and $TB = 484$. The phase plate was a chrome film exposed by E-beam lithography, which reduced the RMS phase error from 17.1° to 6° and changed the typical chirp slope by no more than 0.04 percent out of a total nominal value of 2500 MHz/s. Highest time sidelobes in the compressed pulse were at about −26.8 dB [176].

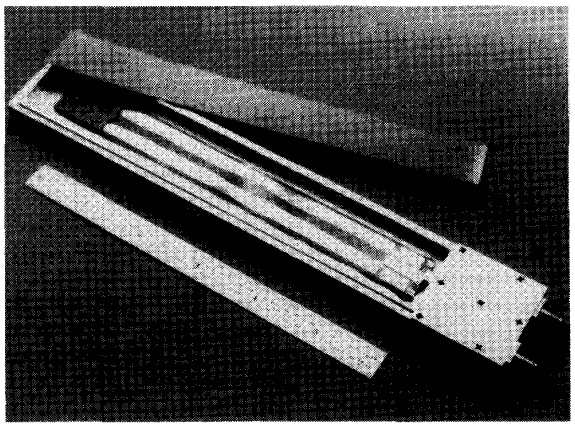

Fig. 9. Photograph of an 80-μs quartz RAC for radar applications (courtesy of SAWTEK, Incorporated, Orlando, FL).

D. SAW Chirp Filters for Nondispersive Delay Lines

Linear FM chirp filters are the most versatile of SAW signal-processing devices. For example, a variable nondispersive delay line was invented at an early date using two cascaded linear FM SAW chirp filters and mixers operating with spectral inversion [177]. This technique has been used in the 70-MHz IF stages of a satellite communications link to provide adaptive cancellation of multipath signals arriving at the receiver up to 30 μs after the direct signal [178]. Two down-chirp RACs were employed in the variable delay line. The input RAC had $TB = 1200$ with $T = 60\ \mu s$, while the output one had $TB = 300$, with $T = 30\ \mu s$ [178].

E. SAW Chirp Structures for Broad-Band Filters

Linear-phase SAW-filter operation can be realized with equal input and output chirp IDTs laid down with the same frequency-time slope [170]. This can be particularly useful in large bandwidth designs, such as in 70-MHz IF stages of satellite ground-station receivers requiring bandwidths up to BW = 50 percent. Delay lines with octave bandwidth (i.e., BW = 66 percent) are also reported using slanted chirp filters on Y-Z $LiNbO_3$ with 2–10-μs delay, 140-MHz bandwidth, and up to ±0.1-dB passband flatness [179]. By using in-line SAW chirp transducers with cubic rather than quadratic phase response, delay lines with greater than 100-percent fractional bandwidth have been fabricated on Y-Z $LiNbO_3$, with 39-dB unmatched insertion loss [180].

VIII. Coding Using SAW Transversal Filters

A. Matched Filtering Versus Correlation

Matched filtering of a data bit provides a completely asynchronous method of demodulation, with a continuous output in time that represents all relations between signal and reference codes. Correlation, on the other hand, furnishes only one output sample at a time as a particular value of the relationship between signal and reference [181].

SAW-based matched filtering can be implemented using fixed or programmable transversal filters (PTFs) for modest processing gains PG = N, where N is the number of bits or chips in the coding waveform. Applications include a) matched filters in spread-spectrum communications and radar, b) adaptive filters for interference mitigation, c) channel equalization in microwave digital radio, and d) radar simulation [40].

B. Barker-Coded SAW Transversal Filters

Barker codes are biphase codes with equal-amplitude time-sidelobes with peak-to-sidelobe ratios (PSR) of $20.\log(N)$ dB under pulse compression, where N is the number of code bits. In pulse-compression radar, these PSR values will, of course, decrease away from the zero-doppler axis [183]. Pure Barker codes have maximum length $N = 13$. Communications applications include use in search radars

where increased range resolution and ranging accuracy are required; as well as for improving sub-clutter visibility, while using pulse lengths suitable for detection.

Combined Barker codes are obtained by further encoding each Barker bit N_a with a faster Barker code of chip length N_b. While this gives a processing gain PG = 10.log(N_aN_b), peak-sidelobe ratios with unweighted codes remain at PSR = 20 log(N_a) [182]. It has been demonstrated, however, that values of PSR for Barker codes can be increased by weighting the sidelobes in the energy density spectrum of the autocorrelation function. This is achieved by including a reciprocal-ripple filter in the SAW-filter design [184]. Using this technique, an N = 13 Barker-coded IDT (unweighted PSR = 22.3 dB) on quartz was modified to yield sidelobe suppression of over 28 dB, using frequency-domain analysis and the inverse discrete Fourier transform to calculate the tap weights [185].

C. SAW IDTs For Quadraphase Codes

Quadraphase-coded waveforms can be employed to reduce excessive radar spectral splatter that can result using biphase Barker-code modulation [186]. Barker codes can readily be converted to quadraphase ones for SAW IDT implementation. In this way, a SAW device on ST-quartz with IDT geometries for 13-bit Barker-quadraphase conversion yielded a PSR ≥ 21 dB [187]. Studies of PSR reduction using reciprocal-ripple filters have also been reported for 5 × 5 combined Barker codes with quadraphase IDT geometries on ST-quartz [188].

D. Minimum Shift Keying (MSK)

In spread-spectrum systems employing minimum shift keying (MSK)—also known as continuous phase-shift modulation (CPSM)—transmissions are in the form of contiguous signals at one of two frequencies $f_{1,2} = f_0 \pm (NR/4) = f_0 \pm (1/4T_c)$, where f_0 is the center frequency, N is the number of chips/message bit, R is the message bit rate, and T_c is the chip time. The power spectrum of MSK has higher sidelobe suppression of sidelobes (23 dB) than for biphase modulation, thereby causing less cross-modulation or interference. Moreover, the main lobe of the MSK power spectrum contains 99.5 percent of the MSK energy, compared with 92 percent for binary phase-shift coding.

Using SAW technology, the MSK sequence can be readily generated by applying either a biphase-coded input sequence [189] or a coded impulse one [190] to an MSK-coded SAW IDT. Using the latter technique, an MSK generator using an IDT with sine (not sinc) apodization, operated at f_0 = 300 MHz with N = 127 chips per message bit at rate R = 91 Mbit/s, with T_c = 10.8 nS [190].

E. Programmable Coding with SAW Transversal Filters

Design constraints on TB product, dynamic range, tap numbers, and accuracy may require the use of hybrid programmable transversal filters for handling coded waveforms, rather than fixed-tap filters. One method reported employed by Hazeltine is based on large-scale-integration/SAW (LSI/SAW) techniques [40]. In a Texas Instruments hybrid design, the IDT is physically separate from the control electronics [191]. Here, dual-gate field-effect transistors can be connected to either SAW IDT bus bar for "1", "0" code selection, or none. Tap switching times are about 100 ns. This has been demonstrated for a programmable 16-chip coded IDT on lithium niobate, with SAW sampling rate of 200 MHz. Over 40 dB of tap weight was provided by the IDTs. In adaptive filter operation, a 12-MHz passband could be provided about a center frequency tunable from 200 MHz to 300 MHz [191]. In an MIT Lincoln Laboratory hybrid PTF with a fixed number of fingers (175 or 350) on lithium niobate, the electric fields generated by the surface wave are coupled directly to an adjacent silicon chip with the SiO_2 surface, forming MOS capacitors [192], [193]. Individual MOS capacitances are functions of the bias-voltage applied. These control the level of RF signal coupled from input to output. In this way a device with 350 taps with 30-dB on-off ratios yielded a programmable bandwidth of 100 MHz centered at 175 MHz [192], [193]. Table 6 lists some parameter values for these three hybrid PTFs.

Table 6 Parameters of SAW Hybrid Programmable Transversal Filters (After Ref. [40])

	MIT	TI	Hazeltine
Bandwidth (MHz)	100	100	12.5
Duration (μs)	1.5	0.08	10.2
TB Product	150	8	128
Total Taps	350	16	128
Thermal Dynamic Range (dB)	75	85	50 (73)
Spurious Free Dynamic Range (dB)	—	60	—

As outlined in Fig. 10, PTFs have also been implemented on epitaxial GaAs using a ⟨001⟩-oriented substrate for maximum piezoelectric coupling to the surface waves, and SAW propagation along a (110) direction [52], [194]. The higher

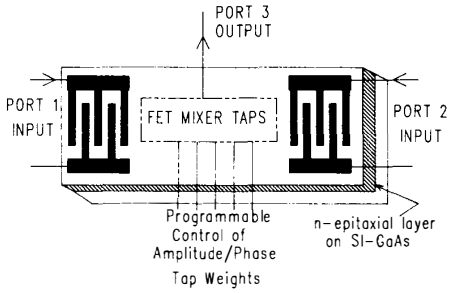

Fig. 10. Geometric outline of a programmable transversal filter on expitaxial GaAs (after Grudkowski, Montress, Gilden, and Black, see [52].

electron-mobility and large bandgap of GaAs provide for operation up to about 1 GHz. The SAW velocity for GaAs is 2868 m/s compared with 3158 m/s for ST-quartz, while K^2 for GaAs is only 38 percent less. The large TCD of +52 ppm/°C for GaAs can be reduced to zero using thin-film overlays.

For PTF operation with the GaAs device, a tapped FET interaction region allows direct interaction with the SAW [39]. This provides milliwatt power dissipation per tap, with high input dynamic range, low spurious signal levels, and large tap on/off ratios. Also, this GaAs device can be configured for operation as a variable phase shifter, a tunable resonator, or for correlation of Barker or biphase codes [52], [194].

IX. SAW Convolvers and Correlators

A. Nonlinear Operation

Three-port and four-port SAW convolvers (configured to act as correlators) have found extensive use in spread-spectrum communications and wide-band radar [46], [195], and more recently in packet-radio systems [48], [196]–[198]. These devices operate in a nonlinear mode under sufficiently high power levels of SAW excitation [199], to correlate a signal under scrutiny with a local reference signal or code in the receiver. The signal contains the code modulation. In contrast to the PTFs considered above, the modulation code can be a lengthy or rapidly-changing one, for large processing gains and/or secure communications. Range resolution, data rates, and processing gain are functions of the signal-coding techniques employed. Because of the limited acoustic penetration depth of a SAW wave, nonlinear operation of SAW-based devices can usually be achieved with much lower signal power levels than for bulk-wave devices. For example, SAW power levels of about 10 mW/mm of acoustic aperture in *Y-Z* lithium niobate represent the upper limit for linear operation at 1 GHz [200].

B. Three-Port SAW Convolvers

Principal commercial three-port SAW convolvers are the monolithic waveguide (also known as an elastic or planar convolver) type of Fig. 11(a) or the acoustoelectric one of Fig. 11(b). Since these devices basically deal with convolution interactions of counter-propagating surface acoustic waves, their operation as correlators requires storage and recall of a time-reversed replica of the original coding signal, which is (normally) recalled in synchronism with the signal under scrutiny.

In these three-port convolvers, the input message signal containing the reference coding is applied to one input port (1), while the reference code is applied to the second input port (2). Both input signals are at the same IF carrier frequency f. Under nonlinear operation, a cross-correlation result is then obtained from the output port (3) at frequency $2f$, from the interaction of the counter-propagating surface waves as measured at an interposed metal electrode. Since these counter-propagating waves are equally affected by temperature variations, oven control of temperature may not be required.

The convolution efficiency η_c of a three-port SAW convolver may be defined as $\eta_c = 10, \log (P_{out}/P_s \cdot P_r)$ dBm^{-1}, where P_{out} is the output power at Port 3, while P_s and P_r are the signal and interaction powers at Ports 1 and 2, respectively. The trend is for P_{out} to be evaluated when $P_s = P_r =$ 0 dBm.

C. Monolithic SAW Convolver

As depicted in Fig. 11(a), convolution efficiency in the monolithic SAW convolver type can be increased by focusing the SAW into an acoustic aperture $W \simeq 2$–$3\,\lambda$ [201]. One technique for achieving this employs a multistrip beamwidth compressor (BWC) [13], [201]. Wide-band BWCs can be designed with loss well under 1 dB [202]. Moreover, diffraction compensation can be applied to the multistrip beam compressors for improved performance [203]. Other SAW focusing methods employ horn compressors, curved IDTs, or narrow-aperture chirp IDTs [26]. Beamwidth

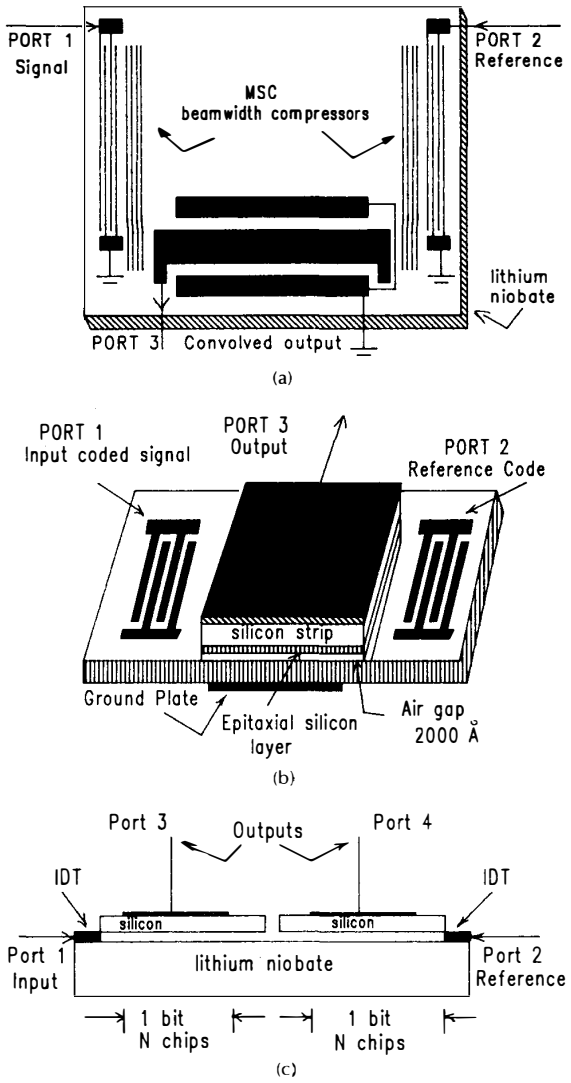

Fig. 11. (a) Outline of 3-port monolithic SAW convolver using MSC beamwidth compression (after Defranould and Maerfeld, see [201].) (b) Three-port acoustoelectric SAW convolver on silicon (after Reible, [45]). (c) Four-port acoustoelectric SAW convolver on silicon. (After Reible, [45]).

compression also serves to suppress spurious transverse acoustic modes which can degrade η_c by adding dispersion and/or reducing time-sidelobes [204].

Ground return planes on either side of the parametric electrode in Fig. 11(a) allow for a single metallization. Moreover, the plate capacitance is independent of the plate width. The Q of the output circuit can then be kept low for wide-band operation. In these structures, a metal waveguide with acoustic aperture $W = 5\,\lambda$ will support three propagating modes at an operating frequency of 300 MHz, while providing operation with large bandwidth and low dispersion [202]. The parametric electrode plate can also have undesirably-large end-to-end resistance up to several hundred ohms, which can reduce output signal levels and also introduce spatial nonuniformities. Compensation for this requires the metal plate to be electrically intercon-

nected by leads attached at a number of places along its length [26].

In some designs on lithium niobate, the length of the parametric electrode may be about one-half of the EM wavelength at the operating frequency. This can lead to standing-wave problems unless the strip is properly terminated [26], [205]. In another design technique, spurious reflections and problems due to self-convolution of the input signal are minimized by using two sets of input IDTs and two convolving parametric electrodes [26].

Monolithic three-port SAW convolvers on $LiNbO_3$ have been reported using beamwidth compressors, curved IDT focusing [206], or small-aperture focused chirp transducers with equal or better performance. The chirp IDT type has yielded a time-bandwidth TB = 1615, with B = 95 MHz referred to the input signals and efficiency $\eta_c = -61$ dBm at midband frequency at 300 MHz [203].

A single-track monolithic convolver has demonstrated a time-bandwidth TB = 2000 on $LiNbO_3$, with B = 100 MHz, interaction time $T = 20$ μs, and $\eta_c = -70$ dBm [207]. With a time duration of 20 μs, operation at code rates of 90 Mchip/s would then allow for the processing of codes up to 1800 chips long. Modeling of the nonlinear response in such designs has been carried out using variational finite-element analysis [208].

D. Three-Port Acoustoelectric SAW Convolver

Figure 11(b) outlines a three-port SAW convolver employing acoustoelectric interactions with an epitaxial silicon layer separated by an air gap of $\simeq 2000$ Å [45], [209]. This design is attractive for very wide-band radar applications. Operating principles differ from the waveguide device in terms of the nonlinear mixing. Here, nonlinear mixing produces second-harmonic voltages across the Si depletion layer [35], [210]. This can be used to obtain an increase in convolution efficiency over the monolithic convolver.

Three-port acoustoelectric SAW convolvers have been engineered to provide input bandwidths up to 100 MHz with processing gains of 30 dB (i.e., TB = 1000), convolution efficiencies $\eta_c \simeq -55$ dBm, and dynamic range exceeding 50 dB. (Typically the dynamic range should be at least 10 dB greater than the processing gain if the effectiveness of the latter is to be realized.) Designs for spread-spectrum communications and wide-band radar have been fabricated for input bandwidths of 200 MHz [195].

E. Four-Port Acoustoelectric SAW Convolver

A four-port SAW convolver is sketched in outline in Fig. 11(c). It contains two segmented silicon elements of equal length. Each will accommodate one message bit containing N chip excursions. This device finds use in spread-spectrum communications, wide-band radar, and packet-radio communications, using MSK modulation (see Section VIII-D) of message signals with differential phase shift keying (DPSK) [45], [211]. Such dual-silicon SAW convolvers have been engineered on $LiNbO_3$ for input bandwidths up to 200 MHz, interaction lengths of 22 μs (two data bits), and time-bandwidth products $TB = 2400$ at IF center frequencies of 500 MHz. Convolution efficiencies are $\eta_c = -68$ to -78 dBm, while the operating temperature range is -25 C° to +75 C°. By combining this convolver with binary-quantized post-processing, waveforms can be processed with a search window of microseconds for a 100-MHz signal, with processing gains in excess of 60 dB [195]. Other spread-spectrum applications of the hybrid correlator include antimultipath processing for data demodulation and ranging. Potential wide-band radar capabilities include 0.75-m range-resolution and 32 Doppler bins for each of 1280 range bins [195].

F. Asynchronous Matched Filtering

Asynchronous matched filtering of long waveforms can be achieved with SAW convolvers in power-limited spread-spectrum systems [48], [195]. Signal and reference waveforms are each required to have a duration of $2T$ for a SAW convolver with interaction time T. Since this requires no gaps in the application of the reference code samples, two SAW convolvers are needed for implementation. Detection of a signal of unknown arrival time is then immediate once it has passed through the correlation interaction area. This technique has been applied to wide-band packet-radio, intended to provide data communications over a wide geographic area [48]. Packet-radio modems have also been demonstrated for a fading environment, using two sets of monolithic SAW convolvers as PTFs with $TB = 64$ and 2000. Data rates were from 1.4 Mb/s down to 44 b/s, with almost ideal tradeoff in signal-processing gain from 18 dB to 61 dB [196]–[198].

Multiple SAW convolvers can also be used to reduce the acquisition time of a direct-sequence (DS) spread-spectrum communications system. This relies on the simultaneous parallel-processing of different subcodes of a longer spreading sequence. It results in a reduction in search time proportional to $M \times N$, where M is the number of chips being processed in each convolver and N is the number of convolvers [212].

Monolithic SAW convolver structures of ZnO-SiO_2-Si with high convolution efficiency have been reported [213]. These structures employed Sezawa wave propagation, and exploited the nonlinearity of the space-charge layer at the silicon surface. Convolution efficiencies $\eta_c = -35$ to -47.5 dBm were obtained in this way [213].

A disadvantage to using the Sezawa mode of propagation in these structures is in the limited bandwidth that can be achieved due to frequency dispersion of the group velocity. The maximum $TB = 227$ obtained experimentally was close to the optimum available value of 320 for $T = 11.5$ μs and $B = 27.9$ MHz about a center frequency of 300 MHz [213].

G. Gap-Coupled SAW Memory Correlators

To date, SAW-based memory correlators have not been able to compete with SAW convolvers in providing TB products of $TB = 2000$ (for $B = 200$ MHz) in wide-band radar and communications systems [214]. Nevertheless, they can find systems applications not handled by the convolver circuitry. Recall that (with SAW convolver operation) the reference code is applied with prior knowledge of the signal to be correlated against. There may be situations, however, where a copy of the signal code is not available to the reference prior to its emission. This is the case for multi-signal sorting and identification. SAW memory correlators may be used to combat this deficiency, since the correlators can be programmed in one half of the carrier signal period, even when the transmitted signal is a single-shot one.

SAW memory correlators can be realized using the

$LiNbO_3$-Si gap-coupled device of Fig. 11(b) [215], or with GaAs-$LiNbO_3$ gap-coupling [214]. Other gap-coupled memory correlators involve two-port variations of Fig. 11(b), where memory storage is achieved using either Schottky diodes [216], [217] or p^+n diodes in a flash mode [218]. The Schottky-diode structure provided eight-channel operation with 40-MHz bandwidth and a 6.5-μs delay in each channel [217].

H. Other SAW Memory Correlators

Monolithic SAW memory correlators on GaAs have been reported on, with potential capability for $TB = 1000$ [219]. When using GaAs, however, lower correlation efficiencies are obtained in wide-band devices unless a piezoelectric film overlay is employed [220]. A large scale monolithic SAW storage correlator/convolver has been reported using ZnO-SiO_2-Si, with highly-oriented ZnO and n-type Si (111), together with an enhancement-mode PI-FET [221]. Correlation/convolution is performed by the FET structure [222]. Higher efficiency is achieved by incorporating piezoelectric oxides in the FET, with self-aligned gates. Devices of this type with 35-mm length and acoustic delays of 10 μs were fabricated for operation at 340 MHz, with insertion loss less than 35 dB and dynamic range greater than 55 dB [221]. Another monolithic correlator using metal-ZnO-SiO_2-Si has ion-implanted depletion in an MOS region of n-type silicon. This structure yielded 3-dB storage times in excess of 0.5 s [220].

I. SAW-Based Acoustooptic Convolvers and Correlators

SAW-based acoustooptic (AO) techniques can be applied to convolution or correlation in spread spectrum receivers [223]–[226]. An AO memory convolver was reported, using the acousto-photorefractive effect to store acoustic signals in $LiNbO_3$. In a "write" operation, a reference waveform $r(t)$ is stored in the SAW region on the $LiNbO_3$, due to refractive index variation when the laser beam is applied [224]. A "read" waveform is then performed by application of another laser beam containing the signal modulation.

An AO convolver on $LiNbO_3$ performed by using double-diffraction of the laser beam or square-law mixing in the detector for the required nonlinearity. Processing gains projected for the AO convolver ranging from 35 to 42 dB, with dynamic ranges from 45 to 52 dB, are about the same as for the AO memory correlator [224]. This structure is outlined in Fig. 13(b).

One-dimensional SAW-based AO correlators are employed in air-borne passive ranging to locate the range of a jamming source. These can operate with bandwidth $B = 100$ MHz, with signal integration over 5 to 20 ms, with time resolution of less than 10 ns [227]. A 2-D AO correlator has also been employed to cover a bandwidth $B = 60$ MHz, with signal integration over a 30-ms period. This device can detect radar returns with S/N ratios of -60 dB, with Doppler resolution of 30 Hz [227].

X. Real-Time SAW Fourier-Transform Processors

A. Transform Processor Types

Three types of SAW-based Fourier-transform processors reviewed here concern a) single-stage processors for real-time spectral or network analysis, b) two-stage processors for cepstrum analysis, and c) two-stage processors for on-line adaptive filtering [49]. Each of these techniques involves signal processing with SAW linear FM chirp filters in receiver IF stages, as outlined in Fig. 12.

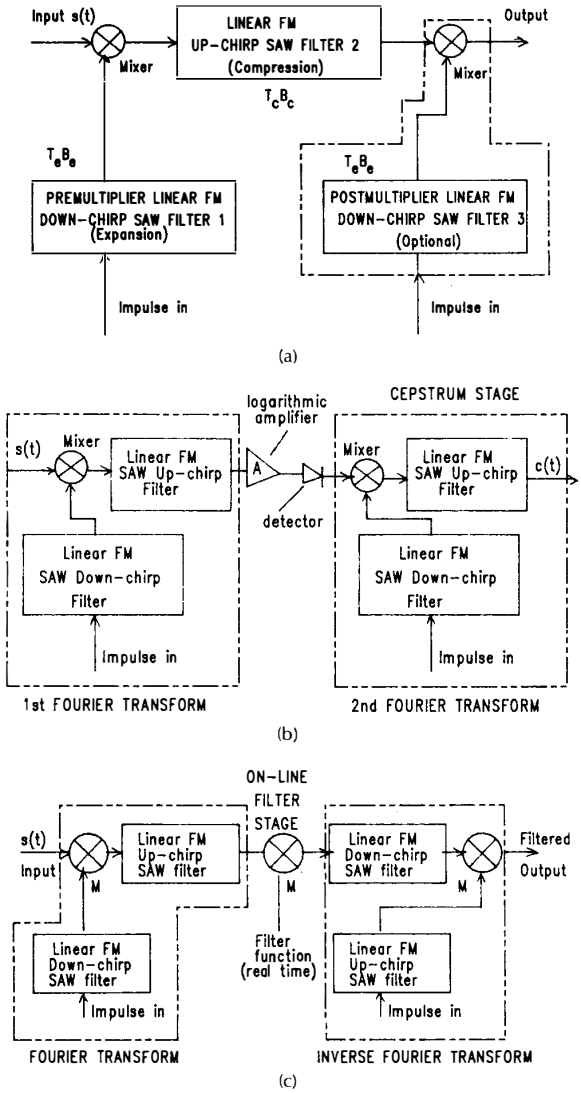

Fig. 12. (a) Real-time M-C-M Fourier-transform processor using three linear FM SAW chirp filters. Configuration here assumes no spectral inversion in mixers. (b) Real-time cepstrum processor employs two Fourier-transform operations and logarithmic amplifier. (c) Real-time adaptive filter capability requires time-gating between Fourier-transform and inverse Fourier-transform stages (after Jack, Grai.., and Collins, [49]).

B. Single-Stage Fourier-Transform Processors

The single-stage transform processors implement a real-time Fourier transform $S(2\pi\mu t)$ operation for real-time spectral or network analysis, where $\mu = B/T$ = magnitude of the linear FM chirp slope. Sonar applications include beam-forming and pulse compression in quasi-real-time passive listening systems as well as sea-bottom imaging [228]. Hybrid

SAW/digital transform processors enjoy a reasonable compatibility for processing signals with bandwidths up to 100 MHz and durations 100–200 μs [228]. In such hybrid systems, for example, up to 100 beams can be employed over the listening band from 10 Hz to 2 kHz. Using SAW chirp filters with bandwidth $B = 40$ MHz and $T = 100\ \mu$s, spectral resolutions of about 2 Hz can be realized over 1000 points [228].

Using three chirp filters with impulse-driven multipliers, as sketched in Fig. 12(a), both the magnitude and phase of the spectral response can be obtained. As shown, this involves a chirp multiplication/convolution/multiplication (M-C-M) operation to yield the Fourier transform. Overall, the chirps perform the Fourier transform $S(2\pi\mu t)$, which can be decomposed as

$$S(2\pi\mu t) = e^{-j\pi\mu t^2} \cdot \left\{ \int_{-\infty}^{+\infty} [s(\tau) e^{j\pi\mu(t-\tau)^2}] \right\} \cdot e^{-j\pi\mu\tau^2}\, d\tau. \quad (4)$$

For simplicity, (4) neglects any mixer spectral inversion or inherent chirp linear-delay terms. The choice of chirp slopes depends on whether or not spectral inversion is used in the mixers. Spectral inversion is employed if down-chirp filters are employed throughout. Post-multiplication is omitted (M-C-(M)) if spectral phase is not required. Relative dispersion times for the multiplier chirp ($T_c B_c$) and the convolver chirp ($T_c B_c$) dictate whether or not meaningful phase data is obtainable.

Real-time SAW-based network analyzers of the M-C-M type can find application in the continuous monitoring of transmission parameters in tropospheric scatter and other communications links, to establish fading patterns [230]. SAW compressive receivers for power spectra only yield a sliding Fourier transform [13], [230]. Optimum spectral coverage occurs when $B_c = 2B_c$ and $T_c B_c = 4T_c B_c$, with the number of resolvable output frequencies $F = T_c B_c$. Processors with large numbers of transform points (e.g., 1024), require RAC chirp filters [49].

A four-channel SAW compressive receiver has been engineered to analyze a 1-GHz signal bandwidth, where each sub-channel had bandwidth $B = 250$ MHz, sample time $T = 250$ ns, as well as a duty cycle of 100 percent. This yielded an overall frequency resolution of $\simeq 4$ MHz, with a time resolution of 500 ns and a 100-percent probability of intercept for a signal duration greater than T. The design used identical chirp filters for both chirp functions in an M-C-(M) structure, with time-grating of the premultiplier chirp to attain the required parameters [231].

The dual transform processor (C)-M-C is employed in some applications. While the M-C-M device can yield better S/N ratio only when magnitude data is required, the C-M-C structure can give better dynamic range since weighting for sidelobe suppression can be included in the compressor, whereas the input to the M-C-(M) structure must be pre-weighted to improve this [231]. However, the additional "expansion loss," due to spectral-energy spreading, must also be considered in the choice of structure [13].

In a (C)-M-C configuration applied to Doppler velocity measurements of moving targets. Doppler resolutions of $\simeq 1.6$ km/h relative to a stationary target were obtained using an infrared laser. The convolving RAC chirp filters had $TB = 400$ with chirp-slope magnitude of 1 kHz/ns, while the multiplier RAC with the same slope had $TB = 900$. The spectral resolution was 84 kHz [232].

The technique can also be extended to perform two-dimensional sonar and radar imaging [228], such as for terrain mapping with synthetic aperture radar. Radar applications include electronic support measures (ESM) for rapid spectral analysis of incoming signals. An application has been described of a digital-in digital-out 512 × 512 point SAW-based transformer for analyzing real-time 4-MHz baseband signals. The digital input is coded into eight complex bits and converted to a real-time signal with 8-MHz bandwidth and 64-μs line time. It is then processed by two SAW Fourier transformers, using chirp filters with TB products $T_1B_1 = 64\ \mu\text{s} \times 8$ MHz and $T_2B_2 = 128\ \mu\text{s} \times 16$ MHz, with 27-dB processing gain [233].

C. Use of SAW Bilinear Mixers

In some Fourier-transform processor designs, it may not be desirable to use conventional double-balanced mixers, since these require one mixer-input level to be held in saturation. SAW bilinear mixers can be employed instead to allow both inputs to be controlled. This allows the input chirp signal (which can be generated digitally) to be amplitude-weighted for reduction of time-sidelobes. One such bilinear mixer on $LiNbO_3$ operated with input signal frequencies of 510 MHz and 838 MHz at signal levels of +23 dBm and +26 dBm, respectively, with a dynamic range greater than 65 dB, acoustic conversion loss of 23 dB and spurious suppression of 33 dB [234].

D. Two-Stage Processors for Cepstrum Analysis

A SAW-based cepstrum processor is outlined in Fig. 12(b). This is composed of two Fourier transformers of Fig. 12(a), separated by a logarithmic amplifier. By definition, the power cepstrum $C(\tau)$ of a time-dependent signal $s(t)$ with spectrum $S(\omega)$ is [235]

$$C(\tau) = |\mathfrak{F}|\,[\log\,|\mathfrak{F}s(t))|^2)]\,|^2 \quad (5)$$

where $\mathfrak{F}$ represents the Fourier-transform operation. For situations where $s(t)$ is distorted by a small periodic echo of amplitude of β and delay τ, the composite power spectrum $|D(\omega)|^2$ is approximated as

$$|D(\omega)|^2 \simeq |S(\omega)|^2 \cdot (1 + 2\beta \cdot \cos(\omega\tau) + \beta^2). \quad (6)$$

Use of the logarithmic amplifier allows the signal and echo product response from the first stage to be separated by the output processor (i.e., $\log(AB) = \log A + \log B$). The output from the second transformer is in the pseudo-time (quefrency) domain, with the dimensions of seconds.

The technique has applications to sonar for real-time separation of echo reverberation, as well as to radar for separating multipath interference. With current RAC chirp filters with time delays of 2 μs to 50 μs and time-bandwidth capability up to $TB = 10\,000$, SAW cepstrum processors have the capability of measuring pulse durations from 50 ns to 50 μs. Other applications include the ability to determine a) the unknown dispersive slope of a radar chirp signal and b) the code length of a binary code or the bit rate, given *a priori* knowledge of one of these parameters [49], [236].

E. Adaptive-Filter Fourier-Processor

While the chirp filters in the first stage of Fig. 12(c) are configured to implement a Fourier transform, those in the second stage yield an inverse Fourier transform. This sep-

aration allows for the inclusion of an intermediate time-gating circuit to perform an on-line filtering function [47], [49], [50], [229]. The intermediate time-gating function $h(t)$ is the impulse response of the desired series notch filter function $H(\omega)$. It can be configured to act as a fixed or adaptive notch filter. This SAW-based technique has an advantage over CCD technology for very wide-band communications with bandwidths $B \geq 100$ MHz [50].

The filtering capability of this real-time SAW transform processor for spread-spectrum communications has been compared with that of a direct sequence (DS) receiver not employing a suppression filter. In one determination, the conventional DS receiver would require a processing gain in the range 255–511, to yield the same probability of error performance with a transform processor with a processing gain of 31 [50].

SAW Fourier-transform processors in systems for anti-jam protection may require a dynamic range of 80 dB to handle variations of input power level [50]. This capability was demonstrated in a SAW spectrum analyzer designed for a 30-MHz instantaneous bandwidth and a resolution better than 100 kHz for an input signal centered at 204 MHz. This yielded a precision of 0.3 dB, with a S/N ratio greater than 70 dB and dynamic range greater than 80 dB [237].

F. Acoustooptic Spectrum Analysis and Computation

As an alternative to the SAW compressive receiver which provides outputs serially in time, SAW-based integrated-optics spectrum analyzers (IOSA) employing SAW Bragg cells find application at input frequencies $\simeq 1$ GHz where there is a close match between SAW and optical fields, with bandwidth capability < 1 GHz [26], [28]. The SAW Bragg cells can be employed in high-speed AO computing systems [38], [238], [239]. In the acoustooptic (AO) spectrum analyzer depicted in Fig. 13(a), the Fourier transform is a spatial one

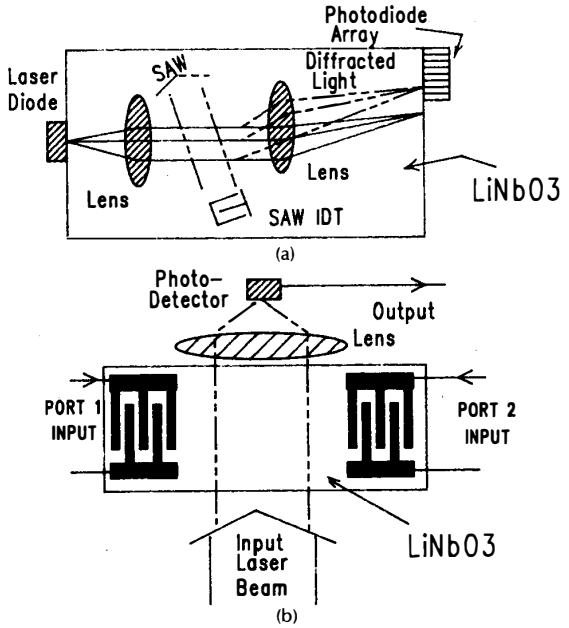

Fig. 13. (a) Outline of acoustooptic spectrum analyzer (after Tsai, [38]). (b) Outline of acoustooptic convolver on $LiNbO_3$ (after Becker, Reible, and Ralston, [224]).

implemented by an optical lens on a piezoelectric surface. Here, light from a laser diode is confined to the surface region by an input planar lens. Bragg diffraction of the light beam then results from its interaction with the periodic refractive index changes due to the SAW from an excited IDT, which can be a chirp one for wide-band operation [240]. The angular distribution of Bragg deflected light is subsequently transformed by the second lens, with a linear array of receiving photodiodes along its focal plane [26], [38].

Most of these devices reported to date have employed $LiNbO_3$ substrates, which only allows for hybrid packaging. Recent studies have been applied to GaAs waveguides for total or monolithic integration with laser diode sources and photodetectors [239].

XI. SAW Oscillators and Frequency Synthesizers

A. SAW Oscillators and Types

SAW oscillators are finding ever-increasing application in precision instrumentation [125], communications, and radar by virtue of their meritorious features of a) high spectral purity, b) fundamental frequency capabilities from 100 MHz to 2 GHz or more, c) small size and weight, and d) low power drain, with maximum RF powers in the range up to $\simeq 20$ dBm. Delay-line or resonator-type SAW oscillators with low vibration sensitivity and aging rates of less than 1 ppm/year offer frequency stabilities comparable with those of low-frequency BAW oscillators, and substantial improvements over multiplied BAW oscillators [125]–[129].

In this paper, SAW oscillators with two-port configurations [131], [132] are grouped into three types according to their design as 1) single-mode fixed-frequency sources, 2) single-mode voltage tunable sources, or 3) those with multimode capability.

B. Single-Mode Fixed-Frequency SAW Oscillators

These find applications as compact frequency sources in precision instrumentation, communications, and radar circuitry. For frequencies below $\simeq 1$ GHz, SAW oscillators using high-Q resonators yield the best stability performance, while SAW oscillators employing delay lines have compatible stability performances at higher frequencies [241].

Low phase-noise performance can be attained using high-quality free-running SAW oscillators. An alternate way of attaining low-noise performance, however, is by injection-locking an oscillator with poor phase noise to a low-noise source. With this technique, the overall noise performance is entirely that of the injection source [242]. An injection-locked SAW oscillator has also been employed as a central component in the design of a UHF FM demodulator with improved FM threshold performance [243].

The aging rate of SAW resonators in SAW oscillators is a function of the operating power level; varying from a few ppm/year to > 1000 ppm/year [244]. Moreover, at power levels above about 20 dBm (depending on the design), excessive resonator surface vibrations will lead to migration of the IDT aluminum metallization, which can cause device failure within a few minutes [245]. This migration can be inhibited to some extent by using an AlCu alloy film rather than pure Al in the IDT metallization [244].

Sources of noise in oscillators include perturbations due to one or more of a) white phase (f^0), flicker phase ($1/f$), white frequency ($1/f^2$), flicker frequency ($1/f^3$), and random walk ($1/f^4$), with frequency-dependent spectral slopes indicated. White frequency and flicker frequency are due to perturbations within the bandwidth of the feedback loop caused by white and flicker phase noise, respectively [246]. Random walk noise relates to long-term aging.

While the predominant noise in most SAW devices is found to be the $1/f$ flicker phase one, SAW resonators are invariably found to also have a $1/f^2$ contribution within 10^{-2} Hz of the carrier frequency [247], [248]. The level of noise in quartz resonators can be dependent on transducer metallization used [249] as well as film stress [250]. SAW devices on $LiNbO_3$ substrates can also exhibit an additional burst noise of varying duration [247].

By way of illustrating high-performance capability, a stabilized 310-MHz SAW oscillator was reported with a noise floor of −176 dBc/Hz at 20 kHz Fourier-frequency offset. This employed a SAW resonator on quartz with $Q = 12\,000$. The acoustic aperture of the resonator was 148 λ_0, while its effective cavity length was 370 λ_0. The large resonator surface area was employed to reduce migrational stress levels in the AlCu IDTs at an operating power level of +20 dBm. The peak stress level of 3.4×10^7 N/m^2 was well inside the high aging level for pure aluminum IDT metallization [127].

The stability performance of SAW oscillators is critically dependent on the inherent temperature sensitivity of the crystal substrate. One way of combating this is to ensure that the crystal is held at a constant temperature in an oven with low thermal time constant. Another technique employs temperature compensation with multiple resonators [251]. A third approach uses a piezoelectric with two SAW delay lines on AT quartz. The delay line with low TCD is employed in the oscillator loop. The other delay line is at an angle to the first, along a high TCD axis. This forms part of a temperature-sensing and microprocessor-control circuit, and adjusts the phase shift around the oscillator loop to compensate for temperature changes. This technique reduced the temperature-induced frequency-dependent variation from ± 125 ppm to ± 1.4 ppm over a temperature range of −23° to 75°C in a system operating at 300 MHz [252].

C. Tunable SAW Oscillators

SAW voltage-controlled oscillators (VCOs) find application in VHF/UHF communications for mobile and cellular radio, where both precision tunability and stability are required over a large number of channels with 12.5-kHz or 25-kHz separation and −70-dB and −80-dB adjacent-channel selectivity. Figure 14 is a photograph of a compact commercial SAW VCO. Most SAW VCOs employ a fixed SAW delay line in series with a voltage-controlled phase shifter in the feedback loop. While quartz is the preferred delay-line substrate, $LiNbO_3$ can be used to reduce the feedback amplifier gain required. Use of this latter substrate requires the feedback loop to be locked to a low-frequency BAW crystal oscillator [256], with a phase-noise multiplier-ratio $20 \cdot \log(n)$ where n is the frequency multiplier ratio [257].

Variable SAW delay lines have also been fabricated with sputtered zinc oxide on an oxidized n-silicon substrate with frequency shift of 560 ppm [253]. Tunable SAW delay lines and two-port resonators are also reported on epitaxial GaAs [52].

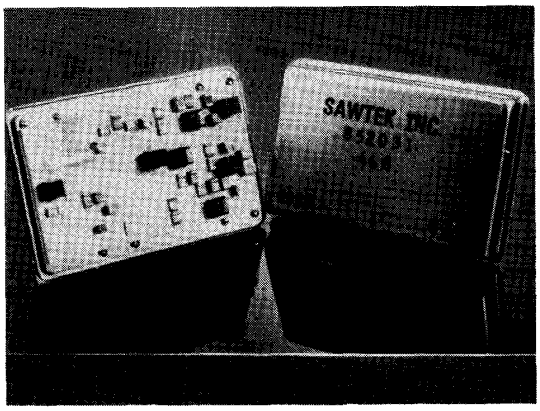

Fig. 14. Photograph of a compact commercial voltage-controlled SAW oscillator (courtesy of SAWTEK, Incorporated, Orlando, FL).

Typical SAW VCO specifications for mobile radio would cater for a tuning range of up to ≃ 1 percent, output power of 4–5 dBm, and a phase noise of −125 dBc/Hz at a Fourier-frequency offset of 10 kHz from the carrier. Thin- or thick-film hybrid constructions can be employed. Thick-film hybrid SAW oscillators have been reported for the frequency range 750–1500 MHz, with frequency settability of ± 10 ppm [254], [255].

Use of a differential SAW delay line with a MOSFET controller in the feedback loop offers a possible improvement in linearity of tuning response over the standard type [258]. Also, a tunable SAW oscillator with three delay lines and a limiter in the feedback loop is reported with a tuning range of about 11.7 percent, with no mode hopping even when the oscillator was tuned over several modes [259].

D. Multimode SAW Oscillators

Multimode oscillators find application in frequency-agile radar. Frequency agility permits decorrelation between radar echoes from successive pulses, as well as a reduction of clutter intensity [260]. A multimode SAW comb oscillator centered around 400 MHz has been described for the local-oscillator stage of a frequency-agile radar. Each comb IDT on the ST-X quartz substrate had 50 rungs spaced by 40 λ_0 with two electrode fingers per rung. This supported 21 comb modes spaced 10 MHz apart (see Section VI-A). Comb-frequency selection was made using a varactor-tuned filter in the feedback loop [164]. Another frequency-selection technique employs temporary forced-injection of the desired frequency, using SAW linear FM chirp filter mixing [261]. Also, low-loss SPUDT-type comb filters can be used in oscillator feedback loops to provide reduced oscillator phase noise over that obtained using "conventional" comb filter counterparts [166].

E. SAW-Based Frequency Synthesizers

A fast frequency-hopping system for spread-spectrum communications has been described which is based on frequency mixing using impulse-driven linear FM chirp filters of opposite slope [262]. The desired CW signal (plus a host of intermodulation products prior to filtering) is obtained as a sum-or-difference mixer output, when the mixer is

driven by the two impulsed chirps. The CW signal is linearly dependent on the time delay between the impulse excitations [262]. A reported system used doubly-dispersive in-line chirp filters on ST-X quartz, with dispersion $T = 10$ μs and chirp slope magnitude $\mu = 4.8$ MHz/s. Fast frequency hopping was obtained at 200 khop/s to any of 240 channels in either of two bands at 356–404 MHz and 306–354 MHz. Potentially, this technique should allow for up to 400-hop frequencies over the 500-MHz bandwidth [262].

Another frequency-synthesis technique employed a comb generator using a step-recovery diode to drive SAW filter banks on ST-quartz, with nine SAW filters per bank over the frequency range 1369–1606 MHz, with tone spacing of 1 MHz and switching speed less than 100 ns [263].

XII. SAW Filters in Digital Communications

A. Systems Components

SAW oscillators and filters are used in many sections of microwave digital radio and satellite digital-communications links [264], [265]. In satellite-communications links using phase-shift-keyed (PSK) digital modulation, they are to be found in the digital modulator (SAW oscillator), bandwidth limiting (SAW filter), and up-converter stages (SAW VCO) in the transmitter, as well as in the down-converter (SAW VCO), noise bandwidth limiting filter (SAW filter), and digital demodulator stages (SAW VCO) of the receiver [264]. In microwave digital radio for the common-carrier bands at 4, 6, and 11 GHz, with bandwidths of 20, 30, and 40 MHz, SAW filters play an important role in spectral-shaping of 70-MHz or 140-MHz IF stages, in conjunction with spectrally-efficient digital-modulation techniques such as quadrature-amplitude-modulation (QAM) [266]–[268]. At this time, 16-QAM and 64-QAM microwave digital radios (employing SAW Nyquist filters) have been engineered, while 256-QAM systems are under development.

In long-haul optical-fiber data-communications links, operating at bit rates from 100 Mbit/s to over 1000 Mbit/s, SAW filters are employed in the clock-recovery circuits for regenerative repeaters, operating at frequencies up to the 1-GHz range [269].

B. SAW Nyquist Filters

Under the Nyquist bandwidth theorem, binary data can be transmitted through an ideal low-pass or linear-phase bandpass channel on an error-free basis (i.e., without inter-symbol-interference (ISI)) at a rate equal to twice the filter cutoff frequency. Practical filters with nonrectangular passband shapes can still transmit with negligible ISI at this rate, however, provided that the filter transition band rolloff is in accord with Nyquist's vestigial symmetry theorem [270]. Typically, this requires a 50 percent excess bandwidth over the ideal one.

Matched filtering requires the Nyquist filter function to be split equally between transmitter and receiver. Moreover, for avoidance of ISI with rectangular pulse trains with $\{(\sin X)/X\}^2$ power spectral distribution, a compensating spectral shaping filter with $X/(\sin X)$ amplitude response is additionally required in the transmitter. Using SAW technology, this spectral-shaping filter can be incorporated with the portion of the Nyquist filter into one composite filter in the transmitter.

Since SAW filters for Nyquist and spectral shaping in microwave digital radio must meet stringent specifications if the bit-error-rate (BER) is to be minimal, this means that bulk-wave interference, diffraction, and IDT end-effects must also be minimized. To this end, some such SAW-filter designs employ V-line IDTs with offset apodization, as shown in Fig. 15, where fingers with short overlaps near the

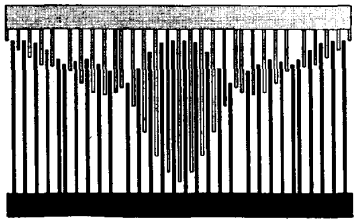

Fig. 15. A V-line IDT with offset apodization. (Reprinted with permission from Vigil, Abbott, and Malocha, [272].)

ends of the IDT have negligible coupling to ground [271], [272].

The use of two weighted IDTs coupled by a multistrip coupler can be advantageous for precision SAW Nyquist filters with large fractional bandwidth. One design for a 70-MHz Nyquist filter with 74-percent bandwidth on 128°-rotated $LiNbO_3$ had amplitude and group delay ripples of 0.2 dB and <10 ns, respectively. The design employed a second-order compensation algorithm which was applicable to IDTs with up to 1000 fingers [273]. A 140-MHz SAW IF filter for a 16-QAM digital radio operating at 140 Mbit/s, with $\simeq$50-MHz bandwidth on 128°-rotated $LiNbO_3$ exhibited negligible ISI [274].

C. Clock Recovery In Optical-Fiber Communications

SAW filters are considered to be the most mature technology available for clock-recovery in regenerators in long-haul optical-fiber communications at data rates from 100 Mbit/s to over 1000 Mbit/s [269]. Practical Q ranges $500 \leq Q \leq 800$ required for these systems dictate the use of transversal filters rather than resonators, with phase-slope ratios of 2 to 3, and a maximum frequency detuning allowance of 0.2 rad [269].

XIII. SAW Antenna Duplexers

Noncirculator types of antenna duplexers consist of transmitter and receiver filters connected in parallel to a common transmit/receive antenna. In mobile and cellular communications, the transmit filter must have low insertion loss with power-handling capability up to 2 W or more. The receive filter must also have low insertion loss as well as good sidelobe suppression. While the receiver SAW filters are readily designed, the problem has been to engineer the SAW transmitter filter to withstand high power levels without breakdown.

SAW-based antenna duplexers are now being employed in UHF portable telephones for cellular radio transceivers [275]. Under EIA standards for Class II portable telephones, they must withstand $\simeq$35-dBm ($\simeq$3.3-W) input power level. These 800-MHz devices are fabricated on a 2×2-mm 36° Y-X $LiTaO_3$ chip, in a TO-5 package. Their insertion loss is about 1–1.2 dB, with output handling powers of up to 2 W.

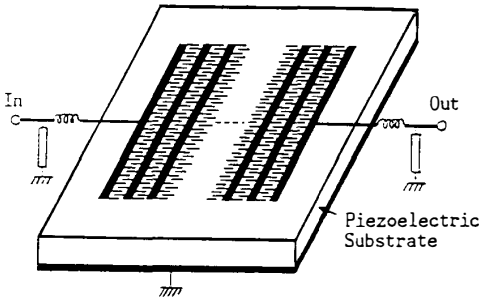

Fig. 16. High-power transmit filter for UHF antenna duplexer uses cascaded SAW resonators. (Reprinted with permission from Hokita, Ishida, Tabuchi, and Kurosawa, [275].)

The high-power transmit filter is constructed with electrically-cascaded SAW resonators as sketched in Fig. 16, with 300–400 IDT finger pairs in each resonator. The resonators themselves are not conventional high-Q types, but wide-band ones operating on a principle similar to that of a laser with distributed feedback [275].

In the above duplexer, metallization of the high-power wide-band resonator filter uses aluminum with 1.5–2.5-percent copper doping [275]. By using sputtered aluminum-titanium (AlTi) metallization with 0.4–0.8-wt percent Ti; however, ladder-type SAW filters for antenna duplexers in mobile telephone transceivers have operated in the range of 3 W at 835 MHz [4].

XIV. SAW Signal Processing on Gallium Arsenide

A. Bias for IDTs on GaAs

While IDTs can be fabricated without modification on semi-insulating GaAs, those deposited on epitaxial GaAs must be biased to form Schottky barriers. Biasing is used to deplete the mobile charge carriers in the region beneath the IDTs so that they do not short out the electrical fields between excited electrodes. With this modification, matched filtering, programmable filtering, or programmable synchronous correlation can be implemented on GaAs with integrated-circuit compatibility [39], [52]. In a reported programmable SAW filter on n-type GaAs, with a carrier concentration of 1×10^{16} cm^{-3}, segmented-FET circuitry was used for tap selection. FET source and drain contacts were ohmic, while the floating gate electrode formed a Schottky barrier. Reversal of the dc bias changed the output phase by 180° [39], [52]. Moreover, in SAW resonator designs on epitaxial GaAs, voltage control of the dc bias on the resonator sections allowed for a tuning capability by controlling the transmission phase through the reflection grating. Such a structure allowed a frequency tuning of 89 ppm in a SAW oscillator for a bias voltage change of 18 V [52]. In another GaAs filter design operating at 300 MHz with bandwidth B = 30 MHz, a quadrature arrangement of two PTFs on the same substrate allowed for control of both the amplitude- and phase-weighting for each tap [276].

B. Acoustic Charge Transfer (ACT) Devices

SAW-based acoustic charge transfer (ACT) devices on epitaxial GaAs have been under intense development in recent years for applications such as to programmable tapped delay lines [277], high-speed sampling, parallel-serial storage, and convolvers [41], [278]. ACT convolver operation is reported with a time–bandwidth product TB = 400, with B = 160 MHz, together with a spurious-free dynamic range of 37 dB and signal-to-noise ratio S/N = 37 dB [279].

Operation of an ACT on GaAs evolves from SAW/CCD devices fabricated on $LiNbO_3$, where the SAW created a travelling potential wave at an adjacent depleted Si surface [280]. Monolithic charge transport SAW devices using metal/ZnO/SiO_2/Si have also been reported [281].

In the illustrative ACT structure of Fig. 17, a metal film plate (biased for Schottky-diode operation) serves as a

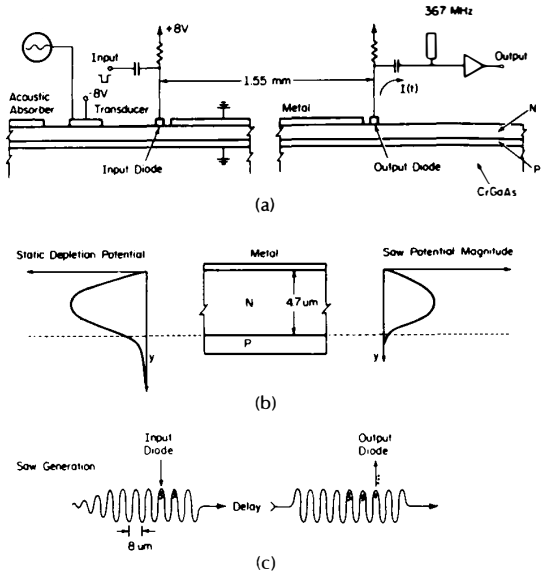

Fig. 17. (a) Side view of ACT structure on GaAs. (b) Transport charge potentials. (c) Charge injection and detection. (Reprinted with permission from Hoskins and Hunsinger, [41].)

charge-transport channel to the output port. In operation, SAW waves from the excited (and biased) input IDT create traveling potential wells at and below the piezoelectric surface, which transport the charges at the SAW velocity [41]. Figure 18 outlines an ACT programmable delay line with

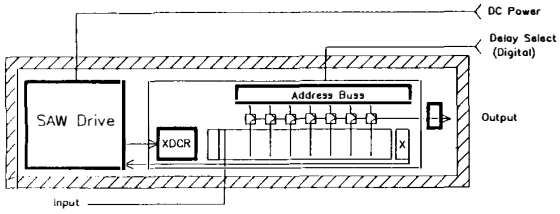

Fig. 18. Schematic of an ACT programmable delay line (courtesyof Electronic Decisions Incorporated, Urbana, IL).

taps to the Schottky transport plate. Such structures can allow for delay ranges of 96 ns to 813 ns in standard products, with up to 128 delay settings at tap spacings of 5.6 ns over bandwidths of B = 150 MHz, with 35-dB spurious-free dynamic range and power consumption < 5 W.

In another ACT design technique, the charge is transported in a heterojunction channel layer of (Al, Ga)As/GaAs/(Al, Ga)As. This ACT has the potential for higher dynamic range, as well as for integrated-circuit compatibility with field-effect transistors [282].

An ACT structure has also been reported using a p-type GaAs transport channel plate on an n-type channel layer. This allowed for the direct optical injection from a 5145-Å laser beam, gated by an acoustooptic modulator [283].

XV. SAW Sensors

A. Sensor Classification

Sensors may be classified within the framework of six categories [44]. These relate to 1) *Measurands* (e.g., acoustic, chemical), 2) *Technological Aspects* (e.g., resolution, sensitivity), 3) *Detection Techniques* (e.g., biological, magnetic), 4) *Sensor Conversion Phenomena* (e.g., biochemical transformation, photoelastic), 5) *Sensor Materials* (e.g., organic, piezoelectric), and 6) *Fields of Application* (e.g., automotive, space). SAW sensors have been engineered to measure, monitor, or control a number of chemical and physical parameters, such as gas concentration [284]–[287], desorption of organic vapors [288], acceleration, stress, and pressure [289]–[291], electrostatic potential [292], magnetic-field strength [293], acoustic absorption [294], and transverse acoustoelectric voltages for nondestructive characterization of semiconductor surfaces [295]. Usually, the parameter under study is determined by causing it to perturb the electric or acoustic characteristics of a SAW delay line in a measurable way. The delay-line perturbations can be measured directly, as for the case of semiconductor surface characterization through a SAW-semiconductor interaction [295].

Where the perturbation effect is very weak, or cannot be measured directly, its level can be deduced from the frequency change produced in a SAW delay-line oscillator. In magnetic-field SAW sensors, for example, the SAW-oscillator frequency sensitivity is 70 Hz/gauss [293]. In acceleration measurements on ST-quartz delay-line oscillators, frequency sensitivities in the order of 10^{-7}/g have been reported [291]. Highlights of some of these techniques are given below.

B. SAW Chemical Gas Sensors

A typical approach to chemical sensing is to cause the gas to alter the frequency of a SAW delay-line oscillator, with sensitivity theoretically increasing with frequency[284]. The aim here is to suitably sensitize the delay-line surface to give maximum change in oscillator frequency, which is usually constrained to be less than 300 MHz. A change of gas concentration causes a change in surface mass. This affects the *acoustic field* of the SAW. It also affects the conductivity of the surface layer and thus the *electric field* of the SAW.

One SAW gas sensor employing this technique uses two isolated delay-line SAW oscillators and ST-X quartz substrates [285]. One of these is affected by the measurement, while the other acts as a reference source. The dual construction thus allows for first-order compensation for temperature, humidity, aging influences, etc. The delay-line surface on the measuring device is coated with a chemical interface in the form of an organic semiconductor (phyhalocyanine) for measuring NO_2 gas concentration. Gas interaction with this surface causes a change in SAW velocity v and delay τ. The frequency difference is then a measure of gas concentration. Sensitivities of $\simeq$100 Hz/ppm NO_2 at an operating frequency of 39.48 MHz were reported, with a threshold sensitivity of about 0.5 ppm [285].

Another dual SAW-oscillator circuit for measuring hydrogen sulphide (H_2S) employed twin SAW delay lines fabricated on a single $LiNbO_3$ substrate. In this case, the sensing SAW delay line was coated with a film of activated tungsten trioxide. This sensor was found to respond to concentrations of H_2S of less than 10 parts per billion [286].

C. Electrostatic Surface Voltage Sensors

To ensure clean copies, electrostatic surface potential measurements are required to monitor and control the electrostatic surface potential of the photosensitive drum in a paper-copying machine. One technique used for this measurement employed an FM-modulated SAW delay-line oscillator [292]. The delay line was on 128° *Y-X* $LiNbO_3$, and incorporated an additional collector electrode driven by a vibrating modulator. The output from an FM demodulator then changed linearly with electrostatic high voltage. This sensor had input impedance over 10^{12} Ω, with high sensitivity and immunity to overload [292].

D. Touch Panel Sensor

An economical touch panel has been reported using SAW absorption. The touch system employs input and output *nondispersive* reflective arrays, for single-frequency operation. This is in conjunction with input and output wedge transducers using thickness-resonant slabs of piezoceramic attached to one side. The reflective arrays cause the output signal to be a composite of all the SAW components having different transit times. Application of a finger to one point of the intermediate surface space causes a dip to appear in the output signal, at a time which is a function of the horizontal position of the touch [294].

E. Acceleration Stress Compensation

Acceleration and vibration can induce stress in a SAW delay line or resonator, and seriously perturb its frequency-response characteristics. This is acceptable, of course, if the aim is to sense these changes. In other SAW oscillator designs, however, it may be necessary to minimize acceleration and vibrational sensitivity. In a SAW device or oscillator subject to acceleration loading, it is thus necessary to have a precise knowledge of the substrate geometry, crystal orientation, and mounting.

In related studies, it is reported that an STC-cut SAW device fabricated on a rectangular plate will have acceleration sensitivities of less than 10^{-9}/g, (in terms of gravitational "g"), expressed as a fractional change in resonant frequency [289], [290].

XVI. SAW Devices in Scanning Acoustic Microscopy

A. SAM and SLAM Microscopes

Scanning acoustic imaging has important applications to the nondestructive testing of microelectronic devices and industrial materials, as well as biomedical diagnosis. Such imaging systems are configured as either scanning laser

acoustic microscopes (SLAM) or scanning acoustic microscopes (SAM) [296]. SAM systems find principal application in the sub-surface imaging of opaque objects [297]. In both of these imaging techniques, distilled water is the most common fluid used for coupling the ultrasound to the area under observation, with an absorption loss of 2.2 dB/mm at 100 MHz at 220 dB/mm at 1 GHz [296].

B. SAM Imaging

A major problem with the SAM imaging technique is in eliminating strong surface reflections from the liquid-surface interface. These can be reduced by operating the SAM in a pulse mode, using RF excitation pulses in conjunction with time-gating to remove spurious echoes [297]. For objects with weak reflectivity, signal-level enhancement can be improved by operating with chirped RF pulses. The pulse-compression SAM operates in analogous fashion to SAW-based pulse-compression radar. Here, the expander waveform passes through an acoustic focusing lens and liquid interface, to the object under study. The reflected signal is then processed by a SAW compressor chirp filter in the receiver. Mechanical or electrical scanning control can be employed.

Using SAW chirp filters with dispersion T and bandwidth B yields a processing gain TB with compressed pulse width $\simeq B^{-1}$. For maximum resolution, therefore, it is desirable to operate with large-bandwidth SAW chirp filters. However, the maximum useful chirp filter bandwidth also depends on the filter center frequency employed. With this limited to about 1 GHz, because of losses in the coupling fluid, the usable bandwidth is about 300 MHz [297].

C. SAW–BAW Mode Conversion Imaging

Experiments are reported on a 100-MHz SAM, where object-scanning for a two-dimensional image relies on a grating scanner. This grating scanner mode-converts surface acoustic waves into bulk acoustic waves to implement a directed beam of acoustic energy. This was achieved by scattering a nonlinear chirped SAW from a curved periodic grating of 350 metal strips on Y-Z $LiNbO_3$ as shown in Fig. 19, to obtain a scanning-line focus of bulk longitudinal

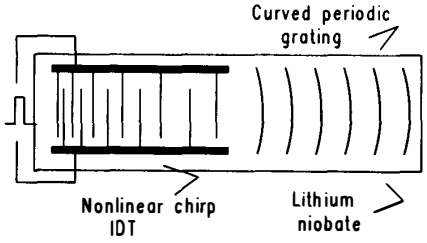

Fig. 19. A SAW-BAW mode-conversion imaging technique for scanning acoustic microscopy at 100 MHz (after Chen, Fu, and Lu, [298]).

waves as a transmitter, with a wide-band bulk probe transducer as a receiver. The SAW nonlinear chirp filter operated around 100 MHz with $T = 1.3\,\mu$s and $B = 50$ MHz. This yielded real-time imaging with a resolution of 70 μm with a scanning velocity $\simeq 3500$ m/s. The field of view was $\simeq 10$ mm with a uniformity better than 1 dB [298]. Two-dimensional acoustic mapping is also reported using a leaky SAW on 128° Y-X $LiNbO_3$ [299].

XVII. Shallow Bulk Acoustic Wave (SBAW) Devices

A. SBAW Requirements and Piezoelectrics

The operation of shallow bulk acoustic wave (SBAW) devices requires efficient propagation of such waves close to the piezoelectric surfaces, as depicted in Fig. 20 [300],

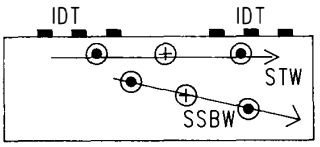

Fig. 20. Illustrating surface skimming bulk wave (SSBW) and surface transverse wave (STW) polarization and propagation.

[301]. To achieve this, the selection of both the piezoelectric and its crystal orientation must satisfy a number of criteria. This includes requirements for large coupling coefficient for the SBAW, zero beam-steering above and below the surface, zero TCD, together with zero (or minimal) coupling to SAW or other bulk waves [42].

Both SBAW and SAW devices employ IDTs. In some instances, the two device types can be visually indistinguishable from one another. For example, operation in one or the other mode on ST-quartz merely involves the choice of a different crystal axis for wave propagation. Moreover, SBAW devices can have a number of relatively attractive features over the SAW ones.

a) SBAW velocities are higher than SAW ones. In 90°-rotated ST-quartz, the SBAW velocity is about 1.6 higher than for SAW. For the same lithographic capability, this increases the device upper-frequency capability by the same factor
b) In some cuts of quartz and $LiTaO_3$, SBAW devices have lower TCD than their SAW counterparts.
c) Since the SBAW propagation is below the piezoelectric surface, this offers reduced sensitivity to surface contamination, as well as better aging performance in oscillator applications.
d) SAW resonators and delay lines can operate at much higher powers than SAW counterparts, before the onset of piezoelectric nonlinearities.
e) Some SBAW devices can have reduced spurious responses.
f) SBAW can have lower propagation loss than SAW at microwave frequencies.

Table 7 is a list of some SBAW crystals and orientations for singly-rotated cuts as shown in Fig. 21(a). Temperature compensation of the 90°-propagating singly-rotated quartz, as well as fine-tuning of device frequency, has been obtained using a thin-film SiO_2 overlay [303].

Doubly-rotated cuts of quartz, with axes shown in Fig. 21(b), have also been examined for SBAW applications, with particular attention to the SC-cut [304]. The doubly-rotated cut is denoted $(YXw1)\phi/\theta$, where the angle ϕ gives an extra degree of freedom and also allows for optimization of other

Table 7 Illustrative SBAW Piezoelectrics and Parameters (After Refs. [43], [302])

Crystal	SBAW Velocity (m/s)	K^2 (%)	Euler Angles			TCD (ppm/°C)
			λ	μ	θ (deg)	
35° rotated *Y*-cut $LiTaO_3$ *X*-prop.	4221	4.7	0	35	0	45
37° rotated *Y*-cut $LiNbO_3$ *X*-prop.	4802	16.7	0	37.93	0	59
Rotated *Y*-cut ST-quartz	4990	1.89	0	132.75	90	33
+35.5° (AT) rotated *Y*-cut quartz	5100	1.44	0	125.15	90	±127 (−55 to +85°C)
−50.5° (*BT*) rotated *Y*-cut quartz	3331	0.4	0	41	90	±55 (−55 to +85°C)

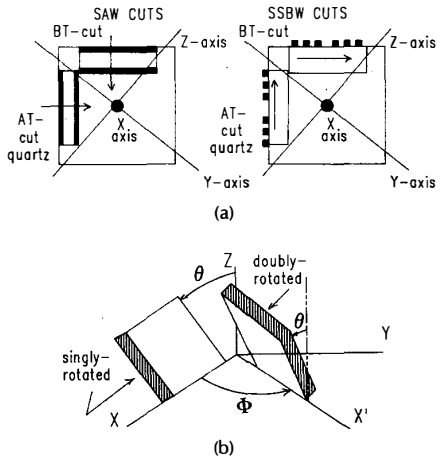

Fig. 21. (a) Rotated-*Y* cuts on quartz for SAW and SSBW use (after Lewis, [42]). (b) Singly- and doubly-rotated crystal cuts (after Ballato and Lukaszek, [304]).

parameters [304]. Berlinite has also been under study for SBAW application.

B. Surface Skimming Bulk Waves Devices

Devices employing SBAW propagation are also referred to as surface skimming bulk wave (SSBW) ones, when no wave-trapping grating is employed between input and output IDTs in Fig. 20 [42], [43]. In modeling the impulse response $h(t)$ of an SBAW filter relative to its SAW counterpart, it has been shown that the two are related by $h(t)_{SSBW} \propto h(t)_{SAW}/\sqrt{t}$, in terms of response time t [42]. For an unapodized SSBW IDT, this yields the same $\{(\sin X)/X\}^2$ power dependence as for a conventional SAW delay line [305].

Antenna theory may be applied to a modeling of the frequency response of the SBAW IDT [42]. One reason for this is that SSBW motion is closely related to that for Love waves, Bluestein-Gulayevwaves, and those on corrugated surfaces [306]. In all of these last-mentioned propagation mechanisms, acoustic energy is confined to the surface region by a slowing mechanism such as a grating or suitable surface layer. In the SSBW device, on the other hand, the surface confinement results from the action of the excited input IDT as an end-fire antenna array, directing the acoustic energy to the output one. The received power varies at $1/R$ in terms of path length R [42].

Also in terms of antenna theory, an equivalent circuit model can be obtained for the radiation resistance of a SSBW IDT and transducer capacitance, which is similar to the "in-line" model used for some SAW devices [42], [43]. A major difference, however, is that the effective coupling of the SSBW is inversely proportional to $\sqrt{N}$, (N = finger pairs), while the coupling is independent of N in the SAW case [43]. Also, SSBW IDTs with split electrodes have been found to be more directive than those using single ones [307].

A problem that can arise in the design of SSBW devices relates to the spurious wave reflections from the sides of the crystal, particularly since the reflectivity of SSBW is high, and it is difficult to damp out reflected waves by using absorbers on the crystal surface. For *BT*-cut quartz, it has been shown that only one propagating wave is reflected from an unmetallized crystal side, since the shear horizontal wave is the slowest one in this crystal. For $LiNbO_3$, two wave components are reflected, since the shear vertical one is the slowest in this medium [308], [309].

Wide-band SSBW delay lines have been reported using a multistrip coupler (MSC) in conjunction with two apodized IDTs on 35° rotated *Y*-cut $LiTaO_3$ and 37° rotated *Y*-cut $LiNbO_3$. These devices had enhanced spurious bulk wave rejection and temperature stability over their SAW counterparts [310]. Unlike a SAW device, however, 100-percent SSBW power transfer is not performed by an MSC. This is due to unequal strengths of symmetric and antisymmetric mechanical vibrational under the MSC strips [311].

The insertion loss of the SSBW device is the sum of three contributions, due to input and output IDTs (as for a SAW device), with an added loss due to acoustic power-spreading [43]. Since the power loss will increase by an additional 3 dB for every doubling of the path length, SSBW devices are not suitable for delays longer than about 100 λ. For shorter delays, insertion-loss performance is comparable with those for SAW filters. SSBW fractional bandwidths BW = 0.3–2 percent on quartz and BW = 15 percent on $LiTaO_3$ have been reported, with insertion loss ≃ 13 dB and sidelobes > 55 dB, with $TCD \simeq 0$ for the first-order and second-order delay coefficients [43].

SBAW delay lines and high-Q oscillators have been reported, using AT-quartz delay lines with IL = 34 dB at 3.1 GHz and fifth-harmonic *BT*-quartz delay lines with IL = 35 dB at 2.2 GHz. The frequency-Q products $fQ \simeq 6.8 \times 10^{12}$ are well above those reported for SAW delay-line devices [302].

C. Use of an Energy-Trapping Grating

Without compensation, energy loss can be excessive in SSBW delay lines and filters for IDT acoustic separations

greater than about 100 λ [304]. Loss reduction can be achieved, however, by use of a surface slowing layer such as a SiO_2 film on rotated *Y*-cut quartz [312], or by an energy-trapping grating or corrugated surface between IDTs [306]. SBAW devices incorporating such trapping structures are referred to as surface transverse wave (STW) ones, when the acoustic wave motion is predominantly shear-horizontal (SH).

Unlike SAW, surface transverse waves can have a controllable depth of propagation into the piezoelectric substrate. This depth of penetration is dependent on the design of the energy-trapping grating. Increasing the metal strip thickness results in trapping the SH wave more closely to the surface, leading to increased diffraction and insertion loss [313], [314].

In these designs, it is desirable to minimize the acoustic power density since the FM noise floor of an oscillator varies inversely with the square root of the oscillator power [313], while the aging performance worsens with increasing power level [244].

STW propagation has been examined on corrugated surfaces, for groove depths h/λ from 0.75–1.37 percent and 501 or 701 grooves [315], as well as with aluminum strip gratings of various height-to-period ratios [313]. STW propagation under a metal-strip grating differs from that under a grooved one [313]. While both the metal strips and grooves slow the SBAW, the metal strips have an additional slowing effect due to the different shear-wave velocities in metal and substrate. This effect is similar to the slowing of a Love wave along a quartz surface with a thin metal film overlay [313]. As well, the loading of the input/output IDT electrodes themselves can affect the shape and mutual positions of the stopbands for the periodic IDT electrodes [316].

D. STW Resonators and Oscillators

Two-port STW resonators employ reflection gratings and an energy trapping grating as sketched in Fig. 22. Here, the period Ω_1 of the electrodes in the reflection gratings is the same as for the IDT fingers. The period Ω_2 of the grating strips corresponds to Ω_2/Ω_1 slightly less than unity.

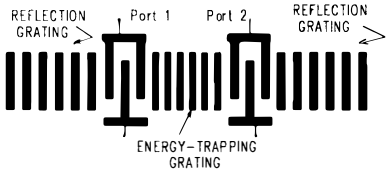

Fig. 22. A two-port STW resonator employing an energy-trapping grating for low-loss operation.

While theoretical *Q*'s as high as 160 000 are predicted for two-port STW resonators on isotropic substrates [318], measured values to date are typically in the 5000 to 10 000 range. Figure 23 shows the measured response of a 1.726-GHz STW resonator on *Y*-rotated quartz, fabricated with *E*-beam lithography and a liftoff process, with linewidth $\simeq 0.74\ \mu$m, reflection grating period $\simeq 1.48\ \mu$m, unloaded $Q \simeq 5600$, and insertion loss 10.27 dB [317]. Packaged STW resonators operating at 500 MHz and 632 MHz showed insertion loss less than 6 dB and *Q*'s as high as 12 000 [317].

Measurements on a 640-MHz *SAW* resonator oscillator operating at a power level of +24 dBm showed an immediate decrease in resonant frequency. A 632-MHz STW resonator operating at +26 dBm, however, showed no appreciable change in *Q* or frequency after 49 days of high-power operation [317]. Flicker phase (1/*f*) noise performance in STW resonators was found to improve with exposure to high operating powers; exhibiting device noise less than −135 dBc/Hz at 1 Hz Fourier-frequency offset. This may be compared with typical 1/*f* noise levels of −115 to −135 dBc/Hz at 1 Hz offset in comparable SAW devices [317].

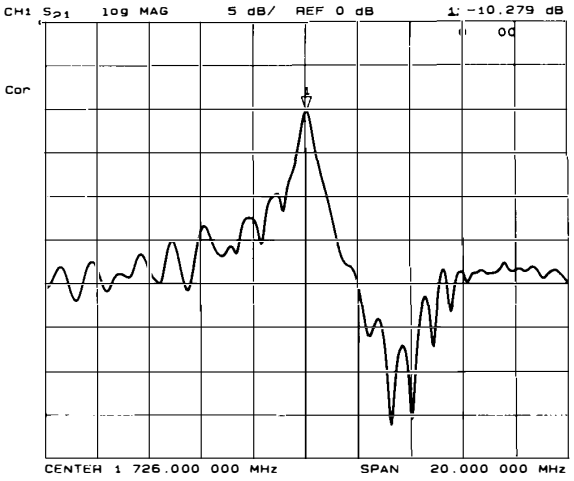

Fig. 23. Transmission response of a 1.726-GHz STW resonator on *Y*-rotated quartz. Fabricated with *E*-beam lithography and lift-off process. Linewidth ~0.74 μm and pitch ~1.48 μm. Q_u ~5600. IL = 10.27 dB. (Reprinted with permission from Bagwell and Bray, [317].)

As with SAW devices, SBAW ones can also be configured to operate in harmonic modes [319], [320]. In demonstration of this, a harmonic group-type STW filter on AT *Y*-rotated quartz was fabricated without sub-micron lithography for operation at the third-harmonic frequency of 1.13 GHz, with insertion loss IL ≃ −26 to −30 dB [321]. It has been shown, however, that the insertion loss of such harmonic STW devices is critically dependent on the thickness of the energy-trapping grating; increasing as much as 50 dB when the grating thickness is increased by a factor of four [322].

XVIII. Discussion

Over a period of 20 years, the SAW-device field has grown into a mature technology extending into numerous areas of electronics and communications. In so doing, the technology has had a substantial influence on RF systems architecture and packaging, such as in the use of hybrid modules. This has led to reductions in systems costs, size, and weight, with particular impact on mobile and portable electronic systems [7]. A recent example of this capability relates to use of SAW devices in secure automobile ignition systems. In one such system, an individually-coded SAW structure is actually embedded in the ignition key. Insertion of the key causes a SAW-encoded signal to be sent to an electronic interrogation module, and then to the engine control computer. Use of the wrong key will prevent the engine from starting up.

SAW technology is now being routinely used for complex

signal-processing techniques in both analog and digital communications systems. The sophistication of both design and fabrication techniques is now such that SAW filters are being built to meet specifications on amplitude and phase response that would have been considered unrealistic just a few years ago [7]. In part this is due to readiness by which many improvements in semiconductor microelectronic fabrication and lithographic techniques can be adapted to the SAW-device field.

SAW-device capability has also been responsible for shifting IF signal processing to significantly higher frequencies than those limited by conventional lumped or distributed inductance-capacitance networks. This is attractive in that it allows for a wider bandwidth capability, as well as for reducing or eliminating spurious mixer signals in IF stages. With their high IF frequency capability, SAW filters will undoubtedly play a vital role in the design and development of IF stages for high-definition TV (HDTV); with first-IF stages operating at, or above, 900 MHz [7].

Another SAW application area which (if successful) could result in a dramatic increase in current production levels relates to the use of SAW transducers as passive elements in electromagnetically-scanned electronic "packaging labels," in locations where optical-scanning cannot be employed or is impractical. In operation, the label package would include a SAW filter with amplitude- or phase-weighted IDTs attached to an RF antenna. In operation, the label is scanned by an EM signal, yielding a re-radiated RF signal that replicates the IDT coding, for label detection.

Shallow bulk acoustic wave (SBAW) device technology is about 10 years younger than that for the SAW field. Already, SBAW devices have proved to be most attractive in competition with SAW ones in areas of resonators and precision oscillators. Given the yardstick of SAW-device development for comparison, the next few years should be important ones for realizing the further potential of SBAW devices.

Acknowledgment

This study was supported in part by an operating grant to the author from the Natural Sciences and Engineering Research Council of Canada.

References

[1] Lord Rayleigh, "On waves propagating along the plane surface of an elastic solid," in *Proc. London Math. Soc.*, vol. 7, pp. 4–11, Nov. 1885.

[2] R. M. White and F. W. Voltmer, "Direct piezoelectric coupling to surface elastic waves," *Appl. Phys. Lett.*, vol. 17, pp. 314–316, 1965.

[3] K. Yamanouchi, Y. Cho, and T. Meguro, "SHF-range surface acoustic wave filters with inter-digital transducers using electron-beam exposure," in *Proc. 1988 IEEE Ultrason. Symp.*, 1988.

[4] J. Yamada, N. Hosaka, A. Yuhara, and A. Iwama, "Sputtered Al–Ti electrodes for high-power durable SAW devices," *Proc. 1988 IEEE Ultrason. Symp.*, 1988.

[5] Y. Ebata and H. Satoh, "Current applications and future trends for SAW in Asia," in *Proc. 1988 IEEE Ultrason. Symp.*, 1988.

[6] R. C. Williamson, "Case studies of successful surface-acoustic-wave devices," in *Proc. 1977 IEEE Ultrason. Symp.*, pp. 460–468, 1977.

[7] C. S. Hartmann, "System impact of modern Rayleigh wave technology," in *Rayleigh-Wave Theory and Application*, E. A. Ash and E. G. S. Paige, Eds. New York: Springer-Verlag, 1985, pp. 236–253.

[8] C. Campbell, *Surface Acoustic Wave Devices and Their Signal Processing Applications*. Boston: Academic Press Boston, 1989.

[9] G. S. Kino, *Acoustic Waves: Devices, Imaging and Analog Signal Processing*. Englewood Cliffs, NJ: Prentice–Hall Inc., 1987.

[10] S. Datta, *Surface Acoustic Wave Devices*. Englewood Cliffs, NJ: Prentice–Hall, 1986.

[11] E. A. Ash and E. G. S. Paige (eds.), *Rayleigh-Wave Theory and Application*. New York: Springer-Verlag, 1985.

[12] A. A. Gerber and A. Ballato (eds.), *Precision Frequency Control*, vol. 1 and vol. 2. New York: Academic Press, Inc., 1985.

[13] D. P. Morgan, *Surface-Wave Devices for Signal Processing*. New York: Elsevier, 1985.

[14] V. M. Ristic, *Principles of Acoustic Devices*. New York: John Wiley & Sons, 1983.

[15] E. Dieulesaint and D. Royer, *Elastic Waves in Solids*. New York: John Wiley & Sons, 1980.

[16] L. M. Brekhovskikh, *Waves in Layered Media*, 2nd Ed. New York: Academic Press, 1980.

[17] A. A. Oliner (ed.), *Acoustic Surface Waves*, Topics in Applied Physics, vol. 24, New York: Springer-Verlag, 1978.

[18] H. Matthews (ed.), *Surface Wave Filters*. New York: John Wiley & Sons, 1977.

[19] J. H. Collins and L. Masotti (eds.), *Computer-Aided Design of Surface Acoustic Wave Devices*. New York: Elsevier, 1976.

[20] B. A. Auld, *Acoustic Fields and Waves in Solids*, vols. 1, 2. New York: John Wiley & Sons, 1973.

[21] Special Issue on Microwave Acoustic Signal Processing, *IEEE Trans. Microwave Theory Tech.*, vol. MTT-21, April 1973.

[22] International Specialist Seminar on "Component Performance and Systems Applications of Surface Acoustic Wave Devices," IEE (Great Britain) Conference Publication Number 109, Sept. 25–28, 1973.

[23] D. P. Morgan (ed.), *Key Papers on Surface-acoustic-wave Passive Interdigital Devices*, IEE (Great Britain) Reprint series 2. Stevenage: Peter Peregrinus Ltd., 1976.

[24] A. J. Slobodnik, Jr., T. L. Szabo, and K. R. Laker, "Miniature surface-acoustic-wave filters," *Proc. IEEE*, vol. 67, pp. 129–146, Jan. 1979.

[25] J. H. Collins and P. M. Grant, "A review of current and future components for electronic warfare receivers," *IEEE Trans. Sonics Ultrason.*, vol. SU-26, pp. 117–125, May 1981.

[26] M. F. Lewis *et al.*, "Recent developments in SAW devices," in *IEE Proc.* (UK), vol. 131, Pt. A, pp. 186–212, June 1984.

[27] M. G. Holland and L. T. Claiborne, "Practical surface acoustic wave devices," in *Proc. IEEE*, vol. 62, pp. 582–611, May 1974.

[28] J. D. Maines and E. G. S. Paige, "Surface-acoustic-wave devices for signal processing applications," *Proc. IEEE*, vol. 64, pp. 639–652, May 1976.

[29] R. M. Hayes and C. S. Hartmann, "Surface-acoustic-wave devices for communications," *Proc. IEEE*, vol. 64, pp. 652–671, May 1976.

[30] G. W. Farnell, "Surface wave reflectors and resonators," *Canadian Elec. Eng. J.*, vol. 1, pp. 3–13, 1976.

[31] D. T. Bell, Jr., and R. C. M. Li, "Surface-acoustic-wave resonators," *Proc. IEEE*, vol. 64, pp. 711–721, May 1976.

[32] W. J. Tanski, "Surface acoustic wave resonators on quartz," *IEEE Trans. Sonics Ultrason.*, vol. SU-26, pp. 93–104, Mar. 1979.

[33] A. J. Slobodnik, Jr., "Surface acoustic waves and SAW materials," *Proc. IEEE*, vol. 64, pp. 581–595, May 1976.

[34] A. A. Oliner, "Waveguides for acoustic surface waves: A review," *Proc. IEEE*, vol. 64, pp. 615–627, May 1976.

[35] G. S. Kino, "Acoustoelectric interactions in acoustic-surface-wave devices," *Proc. IEEE*, vol. 64, pp. 724–748, May 1976.

[36] R. M. White, "Surface elastic waves," *Proc. IEEE*, vol. 58, pp. 1238–1276, 1970.

[37] R. C. Williamson, "Properties and applications of reflective-array devices," *Proc. IEEE*, vol. 64, pp. 702–710, May 1976.

[38] C. S. Tsai, "Guided-wave acoustooptic Bragg modulators for wide-band integrated optic communications and signal processing," *IEEE Trans. Circuits Syst.*, vol. CAS-26, pp. 1072–1098, Dec. 1979.

[39] R. T. Webster and P. H. Carr, "Rayleigh waves on gallium

arsenide," in *Rayleigh-Wave Theory and Application*, E. A. Ash and E. G. S. Paige, Eds. New York: Springer-Verlag, pp. 122–130, 1985.
[40] J. H. Cafarella, "Programmable transversal filters: Applications and capabilities," in *Proc. 1987 IEEE Ultrason. Symp.*, vol. 1, pp. 31–42, 1987.
[41] M. J. Hoskins and B. J. Hunsinger, "Recent developments in acoustic charge transport devices," in *Proc. 1986 IEEE Ultrason. Symp.*, vol. 1, pp. 439–450, 1986.
[42] M. Lewis, "Surface skimming bulk waves, SSBW," in *Proc. 1977 IEEE Ultrason. Symp.*, pp. 744–752, 1977.
[43] K. H. Yen, K. F. Lau, and R. S. Kagiwada, "Recent advances in shallow bulk acoustic wave devices," in *Proc. 1979 IEEE Ultrason. Symp.*, pp. 776–785, 1979.
[44] R. M. White, "A sensor classification scheme," *IEEE Trans. Ultrason. Ferroelec. Freq. Contr.*, vol. UFFC-34, pp. 124–126, Mar. 1987.
[45] S. A. Reible, "Acoustoelectric convolver technology for spread spectrum communications," *IEEE Trans. Sonics Ultrason.*, vol. SU-28, pp. 185–195, May 1981.
[46] A. J. Chatterjee, P. K. Das, and L. B. Milstein, "The use of SAW convolvers in spread-spectrum and other signal-processing applications," *IEEE Trans. Sonics Ultrason.*, vol. SU-32, pp. 745–759, Sept. 1985.
[47] L. B. Milstein and P. K. Das, "Spread spectrum receiver using surface acoustic wave technology," *IEEE Trans. Commun.*, vol. COM-25, pp. 841–847, Aug. 1977.
[48] J. H. Fischer *et al.*, "Wide-band packet radio technology," *Proc. IEEE*, vol. 75, pp. 100–115, Jan. 1987.
[49] M. A. Jack, P. M. Grant, and J. H. Collins, "The theory, design, and applications of surface acoustic wave Fourier-transform processors" *Proc. IEEE*, vol. 68, pp. 229–247, 1980.
[50] L. B. Milstein, "Interference rejection techniques in spread spectrum communications," *Proc. IEEE*, vol. 76, pp. 657–671, June 1988.
[51] M. Feldman, J. Henaff, and M. A. Kirov, "SAW and SSBW propagation in gallium-arsenide," in *Proc. 1981 IEEE Ultrason. Symp.*, vol. 1, pp. 264–267, 1981.
[52] T. W. Grudkowski *et al.*, "Integrated circuit compatible surface acoustic wave devices on gallium arsenide," *IEEE Trans. Microwave Theory Tech.*, vol. MTT-29, pp. 1348–1351, Dec. 1981.
[53] A. J. Slobodnik, Jr. *et al.*, "Lithium tantalate SAW substrate minimal diffraction cuts," *IEEE Trans. Sonics Ultrason.*, vol. SU-25, pp. 92–97, Mar. 1978.
[54] T. Chiba and Y. Togami, "Optical observation of acoustic waves and electrical characteristics in $LiTaO_3$ SAW devices," *IEEE Trans. Sonics Ultrason.*, vol. SU-29, pp. 58–63, Jan. 1982.
[55] W. S. Ishak, C. Flory, and B. A. Auld, "Acoustic modes in lithium tetraborate," in *Proc. 1987 IEEE Ultrason. Symp.*, vol. 1, pp. 241–245, 1987.
[56] F. S. Hickernell, "Zinc oxide films for acoustoelectric device applications," *IEEE Trans. Sonics Ultrason.*, vol. SU-32, pp. 621–629, Sept. 1986.
[57] F. S. Hickernell, "The microstructural characteristics of thin-film zinc oxide for SAW transducers," in *Proc. 1984 IEEE Ultrason. Symp.*, vol. 1, pp. 239–242, 1984.
[58] T. Shiosaki *et al.*, "High-coupling and high-velocity SAW using ZnO and AlN films on a glass substrate," *IEEE Trans. Ultrason., Ferroelec. Freq. Contr.*, vol. UFFC-33, pp. 324–330, May 1986.
[59] K. Tsubouchi and N. Mikoshiba, "Zero-temperature coefficient SAW devices on AlN epitaxial films," *IEEE Trans. Sonics Ultrason.*, vol. SU-32, pp. 634–644, Sept. 1985.
[60] O. Yamazaki, T. Mitsuyu, and K. Wasa, "ZnO thin-film SAW devices," *IEEE Trans. Sonics Ultrason.*, vol. SU-27, pp. 369–379, Nov. 1980.
[61] L. A. Coldren, "Characteristics of zinc-oxide-on-silicon signal processing and storage devices," *Proc. IEEE*, vol. 64, pp. 769–771, May 1976.
[62] T. E. Parker and M. B. Shulz, "SiO_2 film overlays for temperature-stable surface acoustic wave devices," *Appl. Phys. Lett.*, vol. 26, pp. 75–77, 1975.
[63] K. Yamanouchi and S. Hayama, "SAW properties of $SiO_2/128°$ y − x $LiNbO_3$ structure fabricated by magnetron sputtering technique," *IEEE Trans. Sonics Ultrason.*, vol. SU-31, pp. 51–57, Jan. 1984.
[64] R. S. Narayan *et al.*, "Acoustic wave attenuation in berlinite," in *Proc. 1984 IEEE Ultrason. Symp.*, vol. 1, pp. 262–267, 1984.
[65] D. Bailey *et al.*, "An experimental study of the SAW properties of several berlinite samples," in *Proc. 1981 IEEE Ultrason. Symp.*, vol. 1, pp. 341–345, 1981.
[66] F. Hauser *et al.*, "A new nonlinear FM coded EMAT for nondestructive testing of materials," in *Proc. 1981 IEEE Ultrason. Symp.*, vol. 2, pp. 989–991, 1981.
[67] V. M. Ristic, "Magnetomechanical coupling coefficient for periodic EMAT's," *IEEE Trans. Sonics Ultrason.*, vol. SU-29, pp. 229–231, July 1982.
[68] K. Kawashima, "Electromagnetic acoustic wave source and measurement and calculation of vertical and horizontal displacements of surface waves," *IEEE Trans. Sonics Ultrason.*, vol. SU-32, pp. 514–522, July 1985.
[69] J. A. Cooper *et al.*, "Surface acoustic wave interactions with cracks and slots: A noncontacting study using lasers," *IEEE Trans. Ultrason. Ferroelec. Freq. Contr.*, vol. UFFC-3, pp. 462–470, Sept. 1986.
[70] A. Aharoni and K. M. Jassby, "Monitoring surface properties of solids by laser-based SAW time-of-flight measurements," *IEEE Trans. Ultrason. Ferroelec. Freq. Contr.*, vol. UFFC-33, pp. 250–256, May 1986.
[71] D. A. Hutchins, F. Hauser, and T. Goetz, "Surface waves using laser generation and electromagnetic acoustic transducer detection," *IEEE Trans. Ultrason. Ferroelec. Freq. Contr.*, vol. UFFC-33, pp. 478–484, Sept. 1986.
[72] W. S. Gorok, P. J. Vella, and G. I. Stegeman, "Optical probing measurements of surface wave generation and reflection in interdigital transducers in $LiNbO_3$," *IEEE Trans. Sonics Ultrason.*, vol. SU-27, pp. 341–354, Nov. 1980.
[73] H. Engan, "Laser probing of SAW convolver waveguide loss," *IEEE Trans. Sonics Ultrason.*, vol. SU-30, pp. 321–323, Sept. 1983.
[74] ——, "A phase sensitive laser probe for pulsed SAW measurements," *IEEE Trans. Sonics Ultrason.*, vol. SU-29, pp. 281–283, Sept. 1982.
[75] R. F. Milsom, "Bulk wave generation by the IDT," in *Computer-Aided Design of Surface Acoustic Wave Devices*, J. H. Collins and L. Masotti, Eds. New York: Elsevier, pp. 64–81, 1976.
[76] H. Engan, "Excitation of elastic surface waves by spatial harmonics of interdigital transducers," *IEEE Trans. Electron Devices*, vol. ED-16, pp. 1014–1017, 1969.
[77] ——, "High-frequency operation of surface-acoustic-wave multielectrode transducers," *Electron. Lett.*, vol. 10, pp. 395–396, 1974.
[78] ——, "Surface acoustic wave multielectrode transducers," *IEEE Trans. Sonics Ultrason.*, vol. SU-22, pp. 395–401, 1974.
[79] T. L. Szabo, K. R. Laker, and E. Cohen, "Interdigital transducer models: Their impact on filter synthesis," *IEEE Trans. Sonics Ultrason.*, vol. SU-26, pp. 321–333, 1979.
[80] P. M. Naraine and C. K. Campbell, "Gigahertz SAW filters on YZ-lithium niobate without the use of sub-micron line widths," in *Proc. 1984 IEEE Ultrason. Symp.*, vol. 1, pp. 93–96, 1984.
[81] W. R. Smith, "Basics of the SAW interdigital transducer," in *Computer-Aided Design of Surface Acoustic Wave Devices*, J. H. Collins and L. Masotti, Eds. New York: Elsevier, pp. 25–63, 1976.
[82] W. R. Smith and W. F. Pedler, "Fundamental- and harmonic-frequency circuit-model analysis of interdigital transducers with arbitrary metallization ratios and polarity sequences," *IEEE Trans. Microwave Theory Tech.*, vol. MTT-23, pp. 853–864, 1975.
[83] R. F. Mitchell and D. W. Parker, "Synthesis of acoustic-surface-wave filters using double electrodes," *Electron. Lett.*, vol. 10, p. 512, 1974.
[84] I. Streibl *et al.*, "SAW diffraction compensation on yz-lithium niobate," in *Proc. 1983 IEEE Ultrason. Symp.*, pp. 62–65, 1983.
[85] R. H. Tancrell and M. G. Holland, "Acoustic surface wave filters," *Proc. IEEE*, vol. 59, p. 393, 1971.
[86] R. H. Tancrell, "Principles of surface wave filter design," in *Surface Wave Filters*, H. Matthews, Ed. New York: John Wiley & Sons, ch. 3, 1977.

[87] C. S. Hartmann, D. T. Bell, Jr., and R. C. Rosenfeld, "Impulse response model design of acoustic surface-wave filters," *IEEE Trans. Microwave Theory Tech.*, vol. MTT-21, pp. 162–175, April 1973.
[88] W. R. Smith, Jr., "Studies of microwave acoustic transducers and dispersive delay lines," Ph. D. Thesis in Applied Physics, Stanford University, pp. 1–147, 1969.
[89] W. R. Smith *et al.*, "Analysis of interdigital surface wave transducers by use of an equivalent circuit model," *IEEE Trans. Microwave Theory Tech.*, vol. MTT-17, pp. 856–864, Nov. 1969.
[90] ——, "Design of surface wave delay lines with interdigital transducers," *IEEE Trans. Microwave Theory Tech.*, vol. MTT-17, pp. 865–873, Nov. 1969.
[91] Y. Y. Hashimoto *et al.*, "Frequency response measurement for SAW devices based on Fourier analysis of impulse response," *IEEE Trans. Sonics Ultrason.*, vol. SU-32, pp. 76–77, Jan. 1985.
[92] C. M. Panasik and B. J. Hunsinger, "Scattering matrix analysis of surface acoustic wave reflectors and transducers," *IEEE Trans. Sonics Ultrason.*, vol. SU-28, pp. 79–91, Mar. 1981.
[93] P. S. Cross and R. V. Schmidt, "Coupled surface-acoustic-wave resonators," *Bell Syst. Tech. J.*, vol. 56, pp. 1447–1481, 1977.
[94] C. K. Campbell and C. B. Saw, "Analysis and design of low-loss SAW filters using single-phase unidirectional transducers," *IEEE Trans. Ultrason., Ferroelec. Freq. Contr.*, vol. UFFC-34, pp. 357–367, May 1987.
[95] P. M. Smith and C. K. Campbell, "A theoretical and experimental study of low-loss SAW filters with interdigitated interdigital transducers," *IEEE Trans. Ultrason. Ferroelec. Freq. Contr.*, vol. 36, Jan. 1989.
[96] S. M. Ritchie, B. P. Abbott, and D. C. Malocha, "Description and development of a SAW filter CAD system," *IEEE Trans. Microwave Theory Tech.*, vol. 36, pp. 456–466, 1988.
[97] A. Reddy, "Design of SAW bandpass filters using new window functions," *IEEE Trans. Ultrason. Ferroelec. Freq. Contr.*, vol. 35, pp. 50–56, Jan. 1988.
[98] D. C. Malocha and C. D. Bishop, "The classical truncated cosine series functions with applications to SAW filters," *IEEE Trans. Ultrason. Ferroelec. Freq. Contr.*, vol. UFFC-34, pp. 75–85, Jan. 1987.
[99] C. S. Hartmann, "Weighting interdigital surface wave transducers by selective withdrawal of electrodes," in *Proc. 1973 IEEE Ultrason. Symp.*, pp. 423–426, 1973.
[100] M. Yamaguchi, K. Y. Hashimoto, and H. Kogo, "A simple method of reducing sidelobes for electrode-withdrawal SAW filters," *IEEE Trans. Sonics Ultrason.*, vol. SU-26, pp. 334–339, Sept. 1979.
[101] K. R. Laker *et al.*, "Computer-aided design of withdrawal-weighted SAW bandpass filters," *IEEE Trans. Circuits Syst.*, vol. CAS-25, pp. 241–251, 1978.
[102] A. J. Slobodnik, Jr., *et al.*, "Low sidelobe SAW filters using overlap and withdrawal weighted transducers," in *Proc. 1977 IEEE Ultrason. Symp.*, pp. 757–762, 1977.
[103] F. G. Marshall, C. O. Newton, and E. G. S. Paige, "Theory and design of the surface acoustic wave multistrip coupler," *IEEE Trans. Microwave Theory Tech.*, vol. MTT-21, pp. 206–215, Apr. 1973.
[104] ——, "Surface acoustic wave multistrip components and their applications," *IEEE Trans. Microwave Theory Tech.*, vol. MTT-21, pp. 216–225, Apr. 1973.
[105] P. M. Smith and C. K. Campbell, "The design of SAW linear phase filters using the Remez exchange algorithm," *IEEE Trans. Ultrason. Ferroelec. Freq. Contr.*, vol. UFFC-33, pp. 318–323, May 1986.
[106] R. F. Milsom, M. Redwood, and N. H. C. Reilly, "The interdigital transducer," in *Surface Wave Filters*, H. Matthews, Ed. New York: John Wiley & Sons, ch. 2, 1977.
[107] K. C. Wagner and G. Visitini, "Spurious bulk waves in SAW filters with apodized transducers," in *Proc. 1988 IEEE Ultrason. Symp.*, 1988.
[108] R. S. Wagers and R. W. Cohn, "Residual bulk mode levels in (YX1)128° $LiNbO_3$," *IEEE Trans. Sonics Ultrason.*, vol. SU-31, pp. 168–174, May 1984.
[109] C. Flory and M. Tan, "Diffraction minimization in SAW devices using wide aperture compensation," *IEEE Trans. Ultrason. Ferroelec. Freq. Contr.*, vol. 35, pp. 498–502, July 1988.
[110] E. B. Savage and G. L. Matthei, "A study of some methods for compensation for diffraction in SAW IDT filters," *IEEE Trans. Sonics Ultrason.*, vol. SU-28, pp. 439–448, Nov. 1981.
[111] W. R. Mader, C. Ruppel, and E. Ehrmann-Falkenau, "Universal method for compensation of SAW diffraction and other second-order effects," in *Proc. 1982 IEEE Ultrason. Symp.*, vol. 1, pp. 23–28, 1982.
[112] T. Kodama, "Broad-band compensation for diffraction in surface acoustic wave filters," *IEEE Trans. Sonics Ultrason.*, vol. SU-30, pp. 127–136, May 1983.
[113] M. Tan and C. Flory, "Fast computation of SAW diffraction by asymptotic techniques," *IEEE Trans. Ultrason. Ferroelec. Freq. Contr.*, vol. UFFC-34, pp. 93–104, Jan. 1987.
[114] C. Flory and M. Tan, "Compensation of diffraction effects in SAW filters using the uniform asymptotic expansion," *IEEE Trans. Ultrason., Ferroelec. Freq. Contr.*, vol. UFFC-34, pp. 105–113, January 1987.
[115] B. S. Panwar, A. B. Bhattacharya, and E. Dieulesaint, "Transmission-line approach for computation of static capacitance of interdigital transducers in multilayered media," *IEEE Trans. Ultrason. Ferroelec. Freq. Contr.*, vol. UFFC-33, pp. 416–420, July 1986.
[116] F. Palma and P. K. Das, "Acoustoelectric interaction in layered semiconductor," *IEEE Trans. Ultrason. Ferroelec. Freq. Contr.*, vol. UFFC-34, pp. 376–382, May 1987.
[117] G. W. Farnell, "Types and properties of surface waves," in *Acoustic Surface Waves*, Topics in Applied Physics, vol. 24, A. A. Oliner, Ed. New York: Springer-Verlag, ch. 2, 1978.
[118] E. Qian *et al.*, "A modified ZnO film model for calculating elastic and piezoelectric properties," *IEEE Trans. Sonics Ultrason.*, vol. SU-32, pp. 630–633, Sept. 1985.
[119] W. J. Ghijsen and P. M. van den Berg, "A rigorous computational technique for the acoustoelectric field problem in SAW devices," *IEEE Trans. Ultrason. Ferroelec. Freq. Contr.*, vol. UFFC-33, pp. 375–384, July 1986.
[120] C. K. Campbell, Y. Ye, and J. J. Sferrazza Papa, "Wide-band linear phase SAW filter design using slanted transducer fingers," *IEEE Trans. Sonics Ultrason.*, vol. SU-29, pp. 224–228, July 1982.
[121] N. J. Slater and C. K. Campbell, "Improved modeling of wide-band linear phase SAW filters using transducers with curved fingers," *IEEE Trans. Sonics Ultrason.*, vol. SU-31, pp. 46–50, Jan. 1984.
[122] P. M. Naraine and C. K. Campbell, "Wide band linear phase SAW filters using apodized slanted fingers," in *Proc. 1983 IEEE Ultrason. Symp.*, vol. 1, pp. 113–116, 1983.
[123] E. A. Ash, "Surface wave grating reflectors and resonators," in *Proc. 1970 IEEE G-MTT International Microwave Symp.*, pp. 385–386, 1970.
[124] C. S. Hartmann and R. C. Rosenfeld, U.S. Patent 3 886 504, May 1975.
[125] R. C. Bray, "Applications of SAW resonators in high-performance instrumentation," *IEEE Trans. Ultrason., Ferroelec. Freq. Contr.*, vol. 35, pp. 331–341, May 1988.
[126] T. E. Parker and G. K. Montress, "Precision surface-acoustic-wave (SAW) oscillators," *IEEE Trans. Ultrason., Ferroelec. Freq. Contr.*, vol. 35, pp. 342–364, May 1988.
[127] T. E. Parker, "Precision surface acoustic wave (SAW) oscillators," in *Proc. 1982 IEEE Ultrason. Symp.*, vol. 1, pp. 268–274, 1982.
[128] L. L. Pendergrass and L. G. Studebaker, "SAW resonator design and fabrication for 2.0, 2.6 and 3.3 GHz," *IEEE Trans. Ultrason. Ferroelec. Freq. Contr.*, pp. 372–379, May 1988.
[129] J. J. Gagnepain, "Rayleigh wave resonators and oscillators," in *Rayleigh-Wave Theory and Application*, E. A. Ash and E. G. S. Paige, Eds. New York: Springer-Verlag, 1985, pp. 151–172.
[130] M. N. Islam, H. A. Haus, and J. Melngailis, "Bulk radiation by surface acoustic wave propagating under a grating," *IEEE Trans. Sonics Ultrason.*, vol. SU-31, pp. 123–135, Mar. 1984.
[131] W. S. Tanski and H. van de Vaart, "The design of SAW resonators on quartz with emphasis on two-ports," in *Proc. 1976 IEEE Ultrason., Symp.*, pp. 260–265, 1976.
[132] P. S. Cross and S. S. Elliott, "Surface-acoustic-wave resonators," *Hewlett-Packard J.*, vol. 32, Dec. 1981.

[133] H. A. Haus and P. V. Wright, "The analyses of grating structures by coupling-of-modes theory," in *Proc. 1980 IEEE Ultrason. Symp.*, vol. 1, pp. 277–281, 1980.
[134] P. V. Wright, "A coupling-of-modes analysis of SAW grating structures," Ph.D. Thesis in Electrical Engineering, Massachusetts Institute of Technology, Apr. 1981.
[135] C. S. Hartmann *et al.*, "An analysis of SAW interdigital transducers with internal reflections and the application to the design of single-phase unidirectional transducers," in *Proc. 1982 IEEE Ultrason. Symp.*, vol. 1, pp. 40–45, 1982.
[136] P. V. Wright, "The natural single-phase unidirectional transducer: A new low-loss SAW transducer," in *Proc. 1985 IEEE Ultrason. Symp.*, vol. 1, pp. 58–63, 1985.
[137] W. H. Haydl, B. Dischler, and P. Hiesenger, "Multimode SAW resonators—A method to study the optimum performance," in *Proc. 1976 IEEE Ultranson. Symp.*, pp. 287–296, 1976.
[138] D. P. Chen and H. A. Haus, "Analysis of metal-strip SAW gratings and transducers," *IEEE Trans. Sonics Ultrason.*, vol. SU-32, pp. 395–408, May 1985.
[139] C. K. Campbell, "Narrow-band filter design using a staggered multimode SAW resonator," *IEEE Trans. Sonics Ultrason.*, vol. SU-32, pp. 65–70, Jan. 1985.
[140] J. N. Sferrazza Papa, C. K. Campbell, and T. Chu, "Design of a UHF SAW resonator using harmonic-mode excitation," in *Proc. 1983 IEEE Ultrason. Symp.*, pp. 277–279, 1983.
[141] L. A Coldren and R. L. Rosenberg, "Surface-acoustic-wave resonator filters," *Proc. IEEE*, vol. 67, pp. 147–158, Jan. 1979.
[142] P. S. Cross *et al.*, "Very low loss SAW resonators using parallel coupled cavities," in *Proc. 1982 IEEE Ultrason. Symp.*, vol. 1, pp. 284–289, 1982.
[143] W. J. Tanski, "Multipole SAW resonator filters: Elements of design and fabrication," in *Proc. 1981 IEEE Ultrason. Symp.*, vol. 1, pp. 100–104, 1981.
[144] T. F. O'Shea and R. Rosenfeld, "SAW resonator filters with optimum transducer rejection," in *Proc. 1981 IEEE Ultrason. Symp.*, vol. 1, pp. 105–110, 1981.
[145] R. L. Rosenberg and L. A. Coldren, "Scattering matrix approach to SAW resonators," in *Proc. 1976 IEEE Ultrason. Symp.*, pp. 266–271, 1976.
[146] L. A. Coldren, "Characteristics of surface acoustic wave resonators obtained from cavity analysis," *IEEE Trans. Sonics Ultrason.*, vol. SU-24, pp. 212–217, May 1977.
[147] H. A. Haus, "Modes in SAW grating resonators," *J. Appl. Phys.*, vol. 48, pp. 4955–4961, Dec. 1977.
[148] P. S. Cross, "Surface acoustic wave resonator filters using tapered gratings," *IEEE Trans. Sonics Ultrason.*, vol. SU-25, pp. 313–319, Sept. 1978.
[149] P. J. Edmonson, C. K. Campbell, and P. M. Smith, "Narrow-band SAW filters using stepped-resonators with tapered gratings," in *Proc. 1984 IEEE Ultrason. Symp.*, pp. 235–238, 1984.
[150] S. S. Schwartz *et al.*, "SAW resonators on silicon with ZnO limited to IDT regions," in *Proc. 1983 IEEE Ultrason. Symp.*, pp. 280–282, 1983.
[151] Y. Ebata, "Suppression of bulk-scattering loss in SAW resonator with quasi-constant acoustic reflection periodicity," in *Proc. 1988 IEEE Ultrason. Symp.*, 1988.
[152] C. S. Hartmann, J. C. Andle, and M. B. King, "SAW notch filters," in *Proc. 1987 IEEE Ultrason. Symp.*, vol. 1, pp. 131–138, 1987.
[153] R. C. Rosenfeld, R. B. Brown, and C. S. Hartmann, "Unidirectional acoustic surface wave filters with 2 dB insertion loss," in *Proc. 1974 IEEE Ultrason. Symp.*, pp. 425–428, 1974.
[154] K. Shibayama *et al.*, "GHz band SAW filter design using group-type unidirectional transducer," *IEEE Trans. Sonics Ultrason.*, vol. SU-28, pp. 91–95, Mar. 1981.
[155] M. Lewis, "SAW filters employing interdigitated interdigital transducers," in *Proc. 1982 IEEE Ultrason. Symp.*, vol. 1, pp. 104–108, 1982.
[156] C. B. Saw and C. K. Campbell, "Improved design of single-phase unidirectional transducers for SAW filters," in *Proc. 1987 IEEE Ultrason. Symp.*, vol. 1, pp. 169–172, 1987.
[157] K. Yamanouchi, Z. H. Chen, and T. Meguro, "New low-loss surface acoustic wave transducers in the UHF range," *IEEE Trans. Ultrason. Ferroelec. Freq. Contr.*, vol. UFFC-34, pp. 531–539, Sept. 1987.
[158] ——, "GHz-range step-type unidirectional low-loss filters and 5 GHz-range conventional I.D.T. in *Proc. 1986 IEEE Ultrason. Symp.*, pp. 81–84, 1986.
[159] K. Yamanouchi and H. Furuyashiki, "Low-loss SAW filter using internal reflection types of new single-phase unidirectional transducers," in *Proc. 1984 IEEE Ultrason. Symp.*, vol. 1, pp. 68–71, 1984.
[160] M. Takeuchi and K. Yamanouchi, "New types of SAW reflectors and resonators consisting of reflecting elements with positive and negative reflection coefficients," *IEEE Trans. Ultrason. Ferroelec. Freq. Contr.*, vol. UFFC-33, pp. 369–374, July 1986.
[161] M. F. Lewis, "Low loss SAW devices employing single state fabrication," in *Proc. 1983 IEEE Ultrason. Symp.*, vol. 1, pp. 104–108, 1983.
[162] C. K. Campbell and C. B. Saw, "Low-loss SAW filters with 70 dB sidelobes using cascaded and weighted single-phase unidirectional transducers," *Electron. Lett.*, vol. 24, pp. 904–905, 7 July 1988.
[163] S. Matsu-ura, K. Hazamu, and T. Murata, "TV tuning systems with a SAW comb filter," *IEEE Trans. Sonics Ultrason.*, vol. SU-28, pp. 156–161, May 1981.
[164] M. F. Lewis, "Practical frequency source for use in agile radar," *Electron. Lett.*, vol. 21, pp. 1017–1018, Oct. 1986.
[165] C. B. Saw *et al.*, "Multifrequency pulsed injection-locked oscillator using a novel low-loss SAW comb filter," in *Proc. 1986 IEEE Ultrason. Symp.*, pp. 273–276, 1986.
[166] C. B. Saw, "Single-phase unidirectional transducers for low-loss surface acoustic wave devices," Ph.D. Thesis in Electrical Engineering, McMaster University, Hamilton, Ontario, Canada, July 1988.
[167] A. J. Slobodnik, Jr., *et al.*, "A SAW multiplexer using flat exponential filters," *IEEE Trans. Sonics Ultrason.*, vol. SU-28, pp. 50–53, Jan. 1981.
[168] L. P. Solie *et al.*, "A SAW filter bank using hyperbolically tapered transducers," in *Proc. 1988 IEEE Ultrason. Symp.*, 1988.
[169] L. P. Solie and M. D. Wohlers, "Use of a SAW multiplexer in FMCW radar system," *IEEE Trans. Sonics Ultrason.*, vol. SU-28, pp. 141–145, May 1981.
[170] R. C. Williamson, "Reflection grating filters," in *Surface Wave Filters*, H. Matthews, Ed. New York: Wiley, ch. 9,. 1977.
[171] R. C. Williamson and H. I. Smith, "The use of surface-elastic-wave reflection gratings in large time-bandwidth pulse-compression filters," *IEEE Trans. Microwave Theory Tech.*, vol. MTT-21, pp. 195–205, Apr. 1973.
[172] L. P. Solie, "The development of high performance RDA devices," in *Proc. 1979 IEEE Ultrason. Symp.*, pp. 682–686, 1979.
[173] B. Lewis and R. G. Arnold, "Electrode reflectors, directionality, and passband ripple in wideband SAW chirp filters," *IEEE Trans. Sonics Ultrason.*, vol. SU-32, pp. 409–422, May 1985.
[174] H. M. Gerard *et al.*, "The design and applications of highly dispersive acoustic surface-wave filters," *IEEE Trans. Microwave Theory Tech.*, vol. MTT-21, pp. 176–186, Apr. 1973.
[175] H. Gautier and C. Maerfeld, "Current applications and trends of SAW components in France," in *Proc. 1988 IEEE Ultrason. Symp.*, 1988.
[176] S. Jen and C. F. Shaffer, "Phase compensation of L-band slanted transducer dispersive filters," in *Proc. 1986 IEEE Ultrason. Symp.*, vol. 1, pp. 51–57, 1986.
[177] J. Burnsweig, U.S. Patent No. PD71403, 1972.
[178] V. S. Dolat and R. C. Williamson, "A continuously variable delay-line system," in *Proc. 1976 IEEE Ultrason. Symp.*, pp. 419–423, 1976.
[179] H. R. Stocker *et al.*, "Octave bandwidth high performance SAW delay lines," in *Proc. 1980 IEEE Ultrason. Symp.*, vol. 1, pp. 386–390, 1980.
[180] P. Dufilie, "SAW delay line with greater than 100% fractional bandwidth," in *Proc. 1984 IEEE Ultrason. Symp.*, pp. 26–29, 1984.
[181] J. H. Cafarella, "Application of SAW convolvers to spread spectrum communications," in *Proc. 1984 IEEE Ultrason. Symp.*, vol. 1, pp. 121–126, 1984.
[182] D. T. Bell, Jr. and L. T. Claiborne, "Phase code generators and correlators," in *Surface Wave Filters*, H. Matthews, Ed. New York: John Wiley & Sons, ch. 7, 1977.

[183] D. K. Barton, *Modern Radar Systems Analysis*. Norwood, MA: Artech House, 1988.
[184] A. W. Rihaczek and R. M. Golden, "Range sidelobe suppression for Barker codes," *IEEE Trans. Aerosp. Electron. Syst.*, vol. AES-7, pp. 1087–1092, Nov. 1971.
[185] A. Biran, "Low-sidelobe SAW Barker 13 correlator," in *Proc. 1985 IEEE Ultrason. Symp.*, vol. 1, pp. 149–152, 1985.
[186] J. W. Taylor, Jr. and H. J. Blinchikoff, "Quadriphase code—A radar pulse compression signal with unique characteristics," *IEEE Trans. Aerosp. Electron. Syst.*, vol. 24, pp. 156–170, Mar. 1988.
[187] C. R. Vale, "SAW quadraphase code generator," *IEEE Trans. Sonics Ultrason.*, vol. SU-28, pp. 132–136, May 1981.
[188] P. J. Edmonson, C. K. Campbell, and S. F. Yuen, "A study of SAW pulse compression using 5 × 5 Barker codes with quadraphase IDT geometries," in *Proc. 1988 IEEE Ultrason. Symp.*, 1988.
[189] W. R. Smith, "SAW filters for CPSM spread spectrum waveforms," in *Proc. 1980 IEEE National Telecommunications Conf.*, vol. 1, pp. 22.1.1–22.1.6, 1980.
[190] J. H. Goll and D. C. Malocha, "An application of SAW convolvers to high bandwidth spread spectrum communications, *IEEE Trans. Sonics Ultrason.*, vol. SU-28, p. 195–205, May 1981.
[191] C. M. Panasik, "250 MHz Programmable transversal filter," in *Proc. 1981 IEEE Ultrason. Symp.*, vol. 1, pp. 48–52, 1981.
[192] D. E. Oates, D. L. Smythe, and J. B. Green, "SAW/FET programmable transversal filter with 100 MHz bandwidth and enhanced programmability" in *Proc. 1985 IEEE Ultrason. Symp.*, vol. 1, pp. 125–129, 1985.
[193] J. B. Green *et al.*, "Adaptive and matched filtering with a SAW/FET programmable transversal filter," in *Proc. 1986 IEEE Ultrason. Symp.*, vol. 1, pp. 137–141, 1986.
[194] S. W. Merritt, G. K. Montress, and T. W. Grudkowski, "GaAs SAW MESFET programmable asynchronous correlator with complex tap weighting," in *Proc. 1983 IEEE Ultrason. Symp.*, vol. 1, pp. 181–184, 1983.
[195] I. Yao and J. H. Cafarella, "Applications of SAW convolvers to spread-spectrum communications and wideband radar," *IEEE Trans. Sonics Ultrason.*, vol. SU-32, pp. 760–770, Sept. 1985.
[196] J. H. Fischer *et al.*, "Wideband packet radio for multipath environments," *IEEE Trans. Commun.*, vol. 36, pp. 564–576, May 1988.
[197] M. Kowatsch, J. T. Lafferl, and A. Ersoy, "An Application of SAW convolvers to spread-spectrum transmission of packet voice," *IEEE Trans. Sonics Ultrason.*, vol. SU-32, pp. 771–777, Sept. 1985.
[198] K. Kowatsch, "Design of a convolver-based packet voice spread spectrum system," in *Proc. 1984 IEEE Ultrason. Symp.*, vol. 1, pp. 127–131, 1984.
[199] C. F. Quate and R. B. Thompson, "Convolution and correlation in real time with nonlinear acoustics," *J. Appl. Phys.*, vol. 16, pp. 494–496, 1970.
[200] A. J. Slobodnik, Jr., "Materials and their influence on performance," in *Acoustic Surface Waves*, A. A. Oliner, Ed. New York: Springer-Verlag, ch. 6, 1978.
[201] P. Defranould and C. Maerfeld, "A SAW planar piezoelectric convolver," *Proc. IEEE*, vol. 64, pp. 748–753, May 1976.
[202] H. Engan, K. Ingebrigtsen, and A. Rønnekleiv, "On the design of high performance planar surface acoustic wave convolvers," *IEEE Trans. Sonics Ultrason.*, vol. SU-31, pp. 175–184, May 1984.
[203] H. P. Grassl and H. Engan, "Small-aperture focusing chirp transducers vs. diffraction compensated beam compressors in elastic SAW convolvers," *IEEE Trans. Sonics Ultrason.*, vol. SU-32, pp. 675–684, Sept. 1985.
[204] R. D. Colvin and E. J. Charlson, "Multimoding in SAW convolver waveguides," *IEEE Trans. Sonics Ultrason.*, vol. SU-27, pp. 385–388, Nov. 1980.
[205] E. L. Adler, "Spatial uniformity and broadband matching in multiply tapped SAW convolvers," *IEEE Trans. Sonics Ultrason.*, vol. SU-32, pp. 685–689, Sept. 1985.
[206] J. B. Green and G. S. Kino, "SAW convolvers using focused interdigital transducers," *IEEE Trans. Sonics Ultrason.*, vol. SU-30, pp. 43–50, Jan. 1983.
[207] H. Gautier and C. Maerfeld, "Wideband elastic convolver," in *Proc. 1980 IEEE Ultrason. Symp.*, pp. 30–36, 1980.
[208] M. Planat *et al.*, "A finite element analysis of the piezoelectric waveguide convolver," *IEEE Trans. Sonics Ultrason.*, vol. SU-32, pp. 428–439, May 1985.
[209] J. H. Cafarella *et al.*, "Acoustoelectric covolvers for programming matched filtering in spread-spectrum systems," *Proc. IEEE*, vol. 64, pp. 756–759, May 1976.
[210] H. Gautier and G. S. Kino, "A detailed theory of the acoustic wave semiconductor convolver," *IEEE Trans. Sonics Ultrason.*, vol. SU-24, pp. 23–33, Jan. 1977.
[211] J. H. Goll and D. C. Malocha, "An application of SAW convolvers to high bandwith spread spectrum communications," *IEEE Trans. Sonics Ultrason.*, vol. SU-28, pp. 195–205, May 1981.
[212] L. B. Milstein, J. Gevargiz, and P. K. Das, "Rapid acquisition for direct sequence spread-spectrum communications using parallel SAW convolvers," *IEEE Trans. Commun.*, vol. COM-33, pp. 593–600, July 1985.
[213] S. Minagawa *et al.*, "Efficient ZnO-SiO_2-Si Sezawa wave convolver," *IEEE Trans. Sonics Ultrason.*, vol. SU-32, pp. 670–674, Sept. 1985.
[214] R. A. Becker, R. W. Ralston, and P. V. Wright, "Wide-band monolithic acoustoelectric memory convolvers," *IEEE Trans. Sonics Ultrason.*, vol. SU-29, pp. 289–298, Nov. 1982.
[215] J. H. Cafarella, "Surface state acoustoelectric memory-correlator," D.Sc. Thesis in Electrical Engineering, Massachusetts Institute of Technology, 1975.
[216] K. A. Ingebrigtsen, "The Schottky diode acoustoelectric memory and correlator—A novel programmable signal processor," *Proc. IEEE*, vol. 64, pp. 764–771, May 1976.
[217] K. A. Ingebrigtsen, A. Rønnekleiv, and S. Stueflotten, "Memory correlators with multiple input channels," *IEEE Trans. Sonics Ultrason.*, vol. SU-32, pp. 697–706, Sept. 1985.
[218] M. A. El Nokali, "Theory of the p + n diode SAW storage correlator in the flash mode," *IEEE Trans. Sonics Ultrason.*, vol. SU-32, pp. 728–733, Sept. 1985.
[219] R. S. Wagers, "Principles of strip-coupled SAW memory correlators," *IEEE Trans. Sonics Ultrason.*, vol. SU-32, pp. 726–727, Sept. 1985.
[220] S. S. Schwartz, R. L. Gunshor, and R. F. Pierret, "Implanted-isolated SAW storate correlator," *IEEE Trans. Sonics Ultrason.*, vol. SU-32, pp. 707–715, Sept. 1985.
[221] M. E. Motamedi, M. K. Kilcoyne, and R. Aatourian, "Large-scale monolithic SAW convolver/correlator on silicon," *IEEE Trans. Sonics Ultrason.*, vol. SU-32, pp. 663–669, Sept. 1985.
[222] J. B. Green and G. S. Kino, "The SAW-FET signal processor," *IEEE Trans. Sonics Ultrason.*, vol. SU-32, pp. 734–744, Sept. 1985.
[223] M. W. Casseday *et al.*, "Wide-band signal processing using the two-beam surface acoustic wave acoustooptic time integrating correlator," *IEEE Trans. Sonics Ultrason.*, vol. SU-28, pp. 205–212, May 1981.
[224] R. A. Becker, S. A. Reible, and R. W. Ralston, "Comparison of acousto-electric and acousto-optic signal processing devices," *Soc. Photo-Optical Instrumentation Eng. (SPIE)*, vol. 209, Optical Signal Processing for C^3I, 1979.
[225] E. G. H. Lean, J. M. White, and C. D. W. Wilkinson, "Thin-film acoustooptic devices," *Proc. IEEE*, vol. 64, pp. 779–788, May 1976.
[226] P. Le *et al.*, "An integrated optic digital correlator module using both acoustooptic and electrooptic Bragg diffractions in $LiNbO_3$, in *Proc. 1987 IEEE Ultrason. Symp.*, pp. 467–470, 1987.
[227] A. P. Goutzoulis and I. J. Abramovitz, "Digital electronics meets its match," *IEEE Spectrum*, pp. 21–25, Aug. 1988.
[228] H. Gautier and P. Tournois, "Signal processing using surface-acoustic-wave and digital components," *Proc. IEE (Great Britain)*, vol. 127, Pt. F. No. 2, pp. 92–98, Apr. 1980.
[229] C. Atzeni, "Saw signal transform techniques," in *Computer-Aided Design of Surface Acoustic Wave Devices*, J. H. Collins and L. Masotti, Eds. New York: Elsevier, pp. 238–265, 1976.
[230] M. A. Jack *et al.*, "Real time network analyzers based on SAW chirp transform processors," in *Proc. 1976 IEEE Ultrason. Symp.*, pp. 376–381, 1976.
[231] G. L. Moule, R. A. Bale, and T. I. Browning, "A 1 GHz bandwidth SAW compressive receiver," in *Proc. 1980 IEEE Ultrason. Symp.*, vol. 1, pp. 216–219, 1980.

[232] D. Arsenault and V. S. Dolat, "Compact multiple-channel SAW sliding-window spectrum analyzer," in *Proc. 1981 IEEE Ultrason. Symp.*, vol. 1, pp. 220–225, 1981.
[233] H. Gautier and P. Tournois, 'Very fast signal processors as a result of the coupling of surface acoustic wave and digital technologies," *IEEE Trans. Sonics Ultrason.*, vol. SU-28, pp. 126–131, May 1981.
[234] R. D. Colvin, P. H. Carr, and E. J. Charlson, "SAW bilinear mixer," in *Proc. 1979 IEEE Ultrason. Symp.*, pp. 721–724, 1979.
[235] B. P. Bogert, M. J. R. Healy, and J. W. Tukey, "The quefrency alanysis of time series for echoes: Cepstrum, pseudo-autocovariance, cross-cepstrum and saphe cracking," in *Proc. Symposium on Time Series Analysis*, M. Rosenblatt, Ed. New York: Wiley, pp. 209–243, 1963.
[236] M. A. Jack, P. M. Grant, and J. H. Collins, "Waveform detection and classification with SAW cepstrum analysis," *IEEE Trans. Aerosp. Electron. Syst.*, vol. AES-13, pp. 610–618, 1977.
[237] C. Lardat, "Improved SAW chirp spectrum analyzer with 80 dB dynamic range," in *Proc. 1978 IEEE Ultrason. Symp.*, pp. 518–521, 1978.
[238] C. S. Tsai, D. Y. Zhang, and P. Le, "Acousto-optic Bragg diffraction in a $LiNbO_3$ channel-planar composite waveguide with application to optical computing," *Appl. Phys. Lett.*, vol. 47, pp. 549, 1985.
[239] C. J. Lii *et al.*, "Wideband acoustooptic Bragg cells in GaAs waveguide," in *Proc. 1986 IEEE Ultrason. Symp.*, vol. 1, pp. 429–433, 1986.
[240] D. Gregoris and V. M. Ristic, "Wide-band transducer for acousto-optic Bragg deflector," *Canadian J. Phys.*, vol. 63, pp. 195–197, 1985.
[241] R. D. Colvin, "UHF acoustic oscillators," *Microwave J.*, vol. 23, pp. 22–33, Nov. 1980.
[242] C. K. Campbell, P. J. Edmonson, and P. M. Smith, "The phase noise characteristics of a driven SAW oscillator in the threshold vicinity for injection locking," in *Proc. 1985 IEEE Ultrason. Symp.*, vol. 1, pp. 283–286, 1985.
[243] C. K. Campbell, "FM demodulation at UHF frequencies using an injection-locked SAW oscillator," *IEEE Trans. Sonics Ultrason.*, vol. SU-29, pp. 310–316, Nov. 1982.
[244] W. R. Shreve *et al.*, "Power dependence of aging in SAW resonators," in *Proc. 1981 IEEE Ultrason. Symp.*, vol. 1, pp. 94–99, 1981.
[245] W. J. Tanski *et al.*, "A radar system application of an 840-MHz SAW resonator stabilized oscillator," *IEEE Trans. Sonics Ultrason.*, vol. SU-28, pp. 146–150, May 1981.
[246] D. B. Leeson, "A simple model of feedback oscillator noise spectrum," *Proc. IEEE*, vol. 54, pp. 329–330, Feb. 1966.
[247] R. L. Baer, "Phase noise in surface-acoustic-wave filters and resonators," *IEEE Trans. Ultrason. Ferroelec. Freq. Contr.*, vol. 35, pp. 421–425, May 1988.
[248] T. E. Parker, "1/f Phase noise in quartz delay lines and resonators," in *Proc. 1979 IEEE Ultrason. Symp.*, pp. 878–881, 1979.
[249] W. J. Tanski, "The influence of a chrome film bonding layer on SAW resonator performance," in *Proc. 1985 IEEE Ultrason. Symp.*, vol. 1, pp. 253–257, 1985.
[250] R. C. Bray *et al.*, "Annealing behavior and phase noise performance of SAW resonators," in *Proc. 1985 IEEE Ultrason. Symp.*, pp. 247–252, 1985.
[251] K. Hohkawa and S. Yoshikawa, "SAW oscillator construction employing multiple resonators," *IEEE Trans. Sonics Ultrason.*, vol. SU-26, pp. 348–353, Sept. 1979.
[252] W. D. Cowan *et al.*, "A 300-MHz digitally compensated SAW oscillator," *IEEE Trans. Ultrason. Ferroelec. Freq. Contr.*, vol. 35, pp. 380–385, May 1985.
[253] S. Urabe, "Voltage controlled monolithic SAW phase shifter and its application to frequency variable oscillator," *IEEE Trans. Sonics Ultrason.*, vol. SU-29, pp. 255–261, Sept. 1982.
[254] N. A. Howard, "GHz thick film hybrid SAW oscillators," in *Proc. 1983 IEEE Ultrason. Symp.*, vol. 1, pp. 283–286, 1986.
[255] S. Neylon, "Hybrid SAW oscillators," *Microwave J.*, vol. 25, pp. 91–93, Feb. 1982.
[256] C. K. Campbell, J. J. Sferrazza Papa, and P. J. Edmonson, "Study of a UHF mobile radio receiver using a voltage-controlled SAW local oscillator," *IEEE Trans. Sonics Ultrason.*, vol. SU-31, pp. 40–46, Jan. 1984.
[257] W. P. Robins, *Phase Noise in Signal Sources.* London: Peregrinus Press, 1982.
[258] R. I. Amorosi and C. K. Campbell, "Studies of a tunable SAW oscillator using a differential SAW delay line with MOSFET control," *IEEE Trans. Sonics Ultrason.*, vol. SU-32, pp. 574–582, July 1985.
[259] H. A. Mol and P. T. M. van Zeul, "SAW delay line oscillator with extended tuning range," *Electron. Lett.*, vol. 24, pp. 889–898, July 1988.
[260] P. Weissglas and S. Svensson, "Local oscillators for frequency agile systems," *Microwave J.*, pp. 35–38, Jan. 1977.
[261] C. B. Saw *et al.*, "Mode selection in a multimode SAW oscillator using FM chirp mixing signal injection," *IEEE Trans. Ultrason. Ferroelec. Freq. Contr.*, vol. UFFC-35, May 1988.
[262] B. J. Darby and J. M. Hannah, "Programmable frequency-hop synthesizers based on chirp mixing," *IEEE Trans. Sonics Ultrason.*, vol. SU-28, pp. 178–185, May 1981.
[263] A. J. Budreau, A. J. Slobodnik, Jr., and P. H. Carr, "Fast frequency hopping achieved with SAW synthesizers," *Microwave J.*, vol. 25, pp. 71–80, Feb. 1982.
[264] J. Henaff and P. C. Brossard, "Implementation of satellite communication systems using surface acoustic waves," *IEEE Trans. Sonics Ultrason.*, vol. SU-28, pp. 161–172, May 1981.
[265] N. G. Jones, R. A. Moore, and C. J. Huber, "Optimized SAW spectral control filters for digital satellite communication system," *IEEE Trans. Sonics Ultrason.*, vol. SU-28, pp. 173–178, May 1981.
[266] M. Suthers *et al.*, "SAW Nyquist filters for digital radio," in *Proc. 1987 IEEE Ultrason. Symp.*, pp. 117–122, 1987.
[267] G. Waters, "A digital radio noise and interference test set," *Hewlett-Packard J.*, vol. 38, pp. 19–26, July 1987.
[268] M. J. McKissock, "Constellation measurement: A tool for evaluating digital radio," *Hewlett-Packard J.*, vol. 38, pp. 13–17, July 1987.
[269] R. L. Rosenberg *et al.*, "Optical fiber repeatered transmission systems utilizing SAW filters," *IEEE Trans. Sonics Ultrason.*, vol. SU-30, pp. 119–126, May 1983.
[270] See for example, K. Feher, *Digital Communications—Satellite/Earth Station Engineering.* Englewood Cliffs, NJ: Prentice-Hall, 1983.
[271] M. Suthers, *et al.*, "Suppression of spurious SAW signals," in *Proc. 1986 IEEE Ultrason. Symp.*, vol. 1, pp. 37–42, 1986.
[272] A. Vigil, B. P. Abbott, and D. C. Malocha, "A study of the effects of apodized structure geometries on SAW filter parameters," in *Proc. 1987 IEEE Ultrason. Symp.*, vol. 1, pp. 139–144, 1987.
[273] C. Ruppel, E. Ehrmann-Falkenau, and H. R. Stocker, "Compensation algorithm for SAW second order effects in multistrip coupler filters," in *Proc. 1985 IEEE Ultrason. Symp.*, vol. 1, pp. 7–10, 1985.
[274] E. Ehrmann-Falkenau, *et al.*, "SAW-filters for spectral shaping in a 140 mbit/s digital radio system using 16 QAM," in *Proc. 1983 IEEE Ultrason. Symp.*, pp. 17–22, 1983.
[275] M. Hokita *et al.*, "Miniature SAW antenna duplexer for 800-MHz portable telephone used in cellular radio systems," *IEEE Trans. Microwave Theory Tech.*, vol. 36, pp. 1047–1056, June 1988.
[276] S. W. Merritt, G. K. Montress, and T. W. Grudkowski, "GaAs SAW/MESFET programmable asynchronous correlator with complex tap weighting," in *Proc. 1983 IEEE Ultrason. Symp.*, vol. 1, pp. 181–184, 1983.
[277] F. Guediri *et al.*, "Performance of acoustic charge transport programmable tapped delay line," in *Proc. 1987 IEEE Ultrason. Symp.*, vol. 1, pp. 11–14, 1987.
[278] M. J. Hoskins, H. Morkoc, and B. J. Hunsinger, "Charge transport by surface acoustic waves in GaAs," *Appl. Phys. Lett.*, vol. 41 (4), Aug. 1982.
[279] R. W. Miller *et al.*, "Modeled and measured ACT based convolver performance," in *Proc. 1987 IEEE Ultrason. Symp.*, vol. 1, pp. 25–29, 1987.
[280] S. Gaalema, R. J. Schwartz, and R. L. Gunshor, "Acoustic surface wave interaction charge-coupled devices," *Appl. Phys. Lett.*, vol. 29 (2), p. 86, 1976.
[281] T. L. Augustine, R. J. Schwartz, and R. L. Gunshor, "Modeling of charge transfer by surface acoustic wave in a monolithic metal/ZnO/SiO_2/Si system," *IEEE Trans. Electron Devices*, vol. ED-29, p. 1976, 1982.

[282] W. J. Tanski *et al.*, "Heterojunction acoustic charge transport devices on GaAs," *Appl. Phys. Lett.*, vol. 52 (1), pp. 18–20, 1988.
[283] R. L. Miller, J. R. Willhite, and A. Divenere, "Direct optical injection in an ACT channel," in *Proc. 1987 IEEE Ultrason. Symp.*, vol. 1, pp. 15–19, 1987.
[284] W. Wohltjen *et al.*, "Trace chemical vapor detection using SAW delay line oscillators," *IEEE Trans. Ultrason. Ferroelec. Freq. Contr.*, vol. UFFC-34, pp. 172–178, Mar. 1987.
[285] A. Venema *et al.*, "NO_2 gas-concentration measurement with a SAW-chemosensor," *IEEE Trans. Sonics, Ultrason. Freq. Contr.*, vol. UFFC-34, pp. 148–155, Mar. 1987.
[286] J. F. Vetelino, R. K. Lade, and R. S. Falconer, "Hydrogen sulfide surface acoustic wave gas detector," *IEEE Trans. Ultrason. Ferroelec. Freq. Contr.*, vol. UFFC-34, pp. 156–161, Mar. 1987.
[287] R. M. White *et al.*, "Plate-mode ultrasonic sensors," *IEEE Trans. Ultrason. Ferroelec. Freq. Contr.*, vol. UFFC-34, pp. 162–171, Mar. 1987.
[288] S. J. Martin *et al.*, "Isothermal measurements and thermal desorption of organic vapors using SAW devices," *IEEE Trans. Sonics, Ultrason. Freq. Contr.*, vol. UFFC-34, pp. 142–147, Mar. 1987.
[289] S. Locke and B. K. Sinha, "Acceleration stress compensated surface acoustic wave devices," *IEEE Trans. Ultrason. Ferroelec. Freq. Contr.*, vol. UFFC-34, pp. 478–484, July 1987.
[290] B. K. Sinha and S. Locke, "Acceleration of vibration sensitivity of SAW devices," *IEEE Trans. Ultrason. Ferroelec. Freq. Contr.*, vol. UFFC-34, pp. 29–38, Jan. 1987.
[291] D. Hauden, M. Planat, and J. J. Gagnepain, "Nonlinear properties of surface acoustic waves: Applications to oscillators and sensors," *IEEE Trans. Sonics Ultrason.*, vol. SU-28, pp. 342–348, Sept. 1981.
[292] R. Inaba and Y. Kasahara, "An electrostatic voltage sensor using surface acoustic waves," *IEEE Trans. Sonics Ultrason.*, vol. SU-29, pp. 381–385, Nov. 1982.
[293] S. M. Hanna, "Magnetic field sensors based on SAW propagation in magnetic films," *IEEE Trans. Ultrason. Ferroelec. Freq. Contr.*, vol. UFFC-34, pp. 191–194, Mar. 1987.
[294] R. Adler and P. J. Desmares, "An economical touch panel using SAW absorption," *IEEE Trans. Ultrason. Ferroelec. Freq. Contr.*, vol. UFFC-34, pp. 195–201, Mar. 1987.
[295] B. Davari and P. K. Das, "Transient behavior of transverse acoustoelectric voltage and nondestructive characterization of semiconductor surfaces," *IEEE Trans. Sonics Ultrason.*, vol. SU-32, pp. 778–790, Sept. 1985.
[296] L. W. Kessler, "Acoustic microscopy commentary: SLAM and SAM," *IEEE Trans. Sonics Ultrason.*, vol. SU-32, pp. 136–138, Mar. 1985.
[297] M. Nikoonahad, G. Yue, and E. A. Ash, "Pulse compression acoustic microscopy using SAW filters," *IEEE Trans. Sonics Ultrason.*, vol. SU-32, pp. 152–163, Mar. 1985.
[298] W. H. Chen, F. C. Fu, and W. L. Lu, "Scanning acoustic microscope utilizing SAW-BAW conversion," *IEEE Trans. Sonics Ultrason.*, vol. SU-32, pp. 181–188, Mar. 1985.
[299] T. Nomura, S. Shiokawa, and T. Moriizumi, "Measurement and mapping of elastic anisotropy of solids using a leaky SAW excited by an interdigital transducer," *IEEE Trans. Sonics Ultrason.*, vol. SU-32, pp. 235–239, Mar. 1985.
[300] K. H. Yen, K. L. Wang, and R. S. Kagiwada, "Efficient bulk wave excitation on ST quartz," *Electron. Lett.*, vol. 13, pp. 37–38, Jan. 1977.
[301] T. I. Browning and M. F. Lewis, "New family of bulk-acoustic-wave devices employing interdigital transducers," *Electron. Lett.*, vol. 13, pp. 128–130, Mar. 1977.
[302] K. V. Rousseau *et al.*, "High Q, single mode S-band SBAW oscillators," in *Proc. 1982 IEEE Ultrason. Symp.*, vol. 1, pp. 279–283, 1982.
[303] F. Josse, "Temperature dependence of SH-wave on rotated y-cut quartz with SiO_2 overlay," *IEEE Trans. Sonics Ultrason.*, vol. SU-31, pp. 162–168, May 1984.
[304] A. Ballato and T. J. Lukaszek, "Shallow bulk acoustic wave progress and prospects," *IEEE Trans. Microwave Theory Tech.*, vol. MTT-27, pp. 1004–1012, 1979.
[305] T. I. Browning *et al.*, "Bandpass filters employing surface skimming bulk waves," in *Proc. 1977 IEEE Ultrason. Symp.*, pp. 753–756, 1977.
[306] B. Auld, J. Gagnepain, and M. Tan, "Horizontal shear surface waves on corrugated surfaces," *Electron. Lett.*, vol. 12, pp. 650–652, 1976.
[307] T. L. Szabo and E. Cohen, "Shear wave frequency-steered beams from electrode arrays," *IEEE Trans. Sonics Ultrason.*, vol. SU-30, pp. 340–345, Nov. 1983.
[308] P. D. Bloch, E. G. S. Paige, and M. W. Wragg, "On the reflection of surface skimming bulk waves," *IEEE Trans. Sonics Ultrason.*, vol. SU-29, pp. 104–111, Mar. 1982.
[309] P. D. Bloch, E. G. S. Paige, and M. W. Wong, "Design considerations for surface skimming bulk wave devices: Reflection, suppression and encapsulation," *IEEE Trans. Sonics Ultrason.*, vol. SU-31, pp. 77–83, Mar. 1984.
[310] K. H. Yen, K. F. Lau, and R. G. Kagiwada, "Shallow bulk acoustic wave filters," in *Proc. 1978 IEEE Ultrason. Symp.*, pp. 680–683, 1978.
[311] E. G. S. Paige and P. Whittle, "Coupling of surface skimming bulk waves with a multistrip coupler," in *Proc. 1979 IEEE Ultrason. Symp.*, pp. 802–805, 1979.
[312] J. Z. Wilcox and K-H Yen, "Shear horizontal surface waves on rotated y-cut quartz," *IEEE Trans. Sonics Ultrason.*, vol. SU-28, pp. 449–454, Nov. 1981.
[313] D. F. Thompson and B. A. Auld, "Surface transverse wave propagation under metal strip gratings," in *Proc. 1986 IEEE Ultrason. Symp.*, vol. 1, pp. 261–266, 1986.
[314] D. L. Lee, "Analysis of energy trapping effects for SH-type waves on rotated y-cut quartz," *IEEE Trans. Sonics Ultrason.*, vol. SU-28, pp. 330–341, Sept. 1981.
[315] A. Renard, J. Henaff, and B. A. Auld, "SH surface wave propagation on corrugated surfaces of rotated y-cut quartz and berlinite crystals," in *Proc. 1981 IEEE Ultrason. Symp.*, vol. 1, pp. 123–127, 1981.
[316] E. J. Danicki, "Propagation of transverse surface acoustic waves in rotated y-cut quartz substrates under heavy periodic metal electrodes," *IEEE Trans. Sonics Ultrason.*, vol. SU-30, pp. 304–312, Sept. 1983.
[317] T. L. Bagwell and R. C. Bray, "Novel surface transverse wave resonators with low loss and high Q," in *Proc. 1987 IEEE Ultrason. Symp.*, vol. 1, pp. 319–324, 1987.
[318] A. Rønnekleiv, "High Q resonators based on surface transverse waves," in *Proc. 1986 IEEE Ultrason. Symp.*, vol. 1, pp. 257–260, 1986.
[319] D. L. Harmon, F. Josse, and J. F. Vetelino, "Surface skimming bulk waves in y-rotated quartz—Experimental characterization and filter device implementation," in *Proc. 1979 IEEE Ultrason. Symp.*, pp. 791–796, 1979.
[320] K. F. Lau *et al.*, "Further investigation of shallow bulk acoustic waves generated by using interdigital transducers," in *Proc. 1977 IEEE Ultrason. Symp.*, pp. 996–1001, 1977.
[321] R. Hugli, "GHz SAW and STW bandpass filters without submicron geometries using harmonic group type unidirectional transducers," in *Proc. 1987 IEEE Ultrason. Symp.*, pp. 183–187, 1987.
[322] R. L. Baer and C. A. Flory, "Harmonic operating of STW filters," in *Proc. 1988 IEEE Ultrason. Symp.*, 1988.

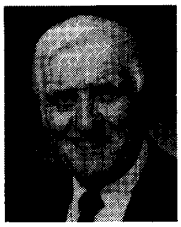

Colin K. Campbell (Fellow, IEEE) was born in St. Andrews, Scotland, in 1927. At the age of 15, during World War II, he trained as a Radio Operator for the British Merchant Navy, and at 17 volunteered for active service with the Royal Corps of Signals, British Army. From 1946 to 1948, he was a Communications Engineer with the Foreign Office, London, England, the British Embassy, Washington, D.C., and the British Delegation to the United Nations, New York. He has also served in the military forces of Canada and from 1962 to 1968 was Commanding Officer of 201 University Squadron, Royal Canadian Air Force.

He attended MIT twice on scholarships, including the Massachusetts Golf Scholarship, and obtained an S.M. degree in electrical engineering there in 1953 for a thesis on power and machines. He also holds an Honors B.Sc. degree in electrical engineering

(1952), a Ph.D. degree in low-temperature physics (1960) from St. Andrews University, Scotland, and a D.Sc. in engineering and applied science (1984) from the University of Dundee, Scotland. As a graduate student in 1959, he was an Invited Member of the British research student delegation at the Meeting of Nobel Physics Prize Winners in Lindau, Bavaria.

An experimentalist by training and inclination, he has conducted research in a wide range of fields, including low-temperature superconductivity, giant-pulse lasers, dielectrics, power-electronic devices, VLSI, millimeter-wave instrumentation, and distributed-parameter devices. He has published numerous papers on SAW devices, as well as a textbook on SAW signal processing.

Dr. Campbell is a Fellow of The Royal Society of Canada, a Fellow of The Engineering Institute of Canada, a Fellow of The Royal Society of Arts (England), and a Member of Sigma Xi. He holds "The Inventor" insignia awarded by Canadian Patents and Development Ltd, as well as three Citations for outstanding contributions to university teaching and education. In 1983, he was the first electrical engineer to be awarded the Thomas W. Eadie Medal of The Royal Society of Canada, for major contributions to engineering and applied science in Canada.

He was with McMaster University, Hamilton, Ontario, Canada, from 1960 to 1989, where he was a Professor of electrical and computer engineering. He is now an independent consultant.